Optical/photonic technology for telecommunication satellites

Department of Electrical and Information Engineering
INDUSTRY 4.0
Ph.D. Program
SSD: ING-INF/02–ELECTROMAGNETIC FIELDS

Final Dissertation

Optical/photonic technology for telecommunication satellites

---

by
Rodio Luca:

Supervisors:

Prof. Giovanna Calò
Prof. Antonella D'Orazio
Dr. Vincenzo Schena

Coordinator of Ph.D. Program:
Prof. Caterina Ciminelli

Course n°36, 01/11/2020-30/01/2024

Department of Electrical and Information Engineering
INDUSTRY 4.0
Ph.D. Program
SSD: ING-INF/02–ELECTROMAGNETIC FIELDS

Final Dissertation

Optical/photonic technology for telecommunication satellites

---

by
Rodio Luca:

Referees:

Prof. Domenico De Ceglia

Prof. Alessandro Vannelli Coralli

Supervisors:

Prof. Giovanna Calò

Prof. Antonella D'Orazio

Dr. Vincenzo Schena

Coordinator of Ph.D Program:
Prof. Caterina Ciminelli

Course n°36, 01/11/2020-30/01/2024

Summary

Introduction

SATellite COMmunications (SATCOM) are changing their paradigm: moving from being a "niche" technology, they are going to enable services much closer to the common consumer experience, as already happened in the past for Internet access and mobile telephony. This translates into new mission scenarios, characherized by the provision of global coverage, increased datarates and connectivity with users and systems that can be also different from those typical of a satellite infrastructure. In this sense the satellite nework can be now conceived as part of an extended "system of systems" providing reliable, performant and secure communication services and opening new market opportunities. This trend is supported by the research efforts of European and national instituions, univerity and industry, which boost the development of those technologies considered enabling for the implementation of such a telecommunication system. In this field optical and photonic technologies play an important role. This thesis work is part of this line of research, with the aim of studying the applicability of optical/photonic technologies on board SATCOM payloads and providing a system demonstration of them. The first part of this thesis document (Chapter 1) provides an introductory onverview on satellite communications. After a summary of its main services and applications, the typical structure of a SATCOM system is described, as well as the main payloads architectures and the orbits taxonomy. Finally current scenarios and future trends for SATCOM are pointed out, with emphasis on High and Very High Throughput Satellite Systems (HTS and VHTS), mega-constellations in Low Earth Orbit (LEO), Space Optical Transport Networks (Space OTNs), micro and nano satellite constellations, which constitute the starting points of the future concept of a full interconnected SATCOM system. The second part (Chapter 2) focuses on optical/photonic technologies. In particular two approaches are proposed for their application on a SATCOM system: the first one is "at payload level", in which some payloads subsystems and the related functionalities are implemented in the optical domain instead of in the microwave/electric one; the second one is "at link level", where optical space-space and space-ground links are exploited instead of the classical RF connectivity. Then, the benefits of both the microwave-photonic technology and the free space optical communication technology are analyzed. Finally the resulting payload architectures are described, namely the hybrid microwave/photonic payload concept and the optical payload concepts, highlighting their differences and commonalities. The last part of this thesis document (Chapter 3, Chapter 4 and Chapter 5) focuses on some of the subsystems/functionalities included in the above payload architectures, in particular hybrid microwave/photonic frequency conversion, optical beamforming for hybrid microwave/photonic payloads and optical circuit switching in free space

optical SATCOM systems. For each of them, after a short technological state-of-the-art overview, a system simulation and performance evaluation is provided.

1.Overview on Satellite Communication

The SATellite COMmunication (SATCOM) industry is experiencing a renewal phase: if in the past decades it was linked mainly to military and institutional missions (e.g. communications in case of emergency, public protection and disaster relief, …) with a limited commercial market such as Direct-To-Home broadcasting (DTH) and sat-phone (satellite phone) communications, nowadays new satellite paradigms are enabling new horizons. This is due to the possibility offered by satellite systems to allow increasingly efficient connectivity, and therefore access to data, in a similar way to what already happens with both wireless and wired terrestrial access infrastructures (e.g. DSL networks, fiber-based networks, Wi-Fi, WiMAX, 5G and beyond networkss, etc.). This development is highly stimulated and supported both by European institutions (European Commission and ESA) and by national and regional ones (in case of Italy ASI, Italian Government, Committee of Italian Regions) since it would support the effective reduction of the Digital Divide in Europe and in the Mediterranean area.

1.1 Services for future SATCOM systems

Telecommunication satellites for commercial and military applications must be able to support a wide range of scenarios, satisfying for each of them the relevant user-side mission requirements and market needs. In first instance the fundamental requirement consists in the provision of a secure and reliable connectivity (e.g. Internet connectivity) to all users. Secondly, within the SATCOM field, there are a series of services, and therefore potential users, linked to those situations in which the terrestrial network infrastructures are not sufficient or are able to guarantee only limited performance (e.g. in terms of capacity) with respect to the user traffic needs.

The main services to be supported by SATCOM systems are:

- **Trunking**: creation of a backbone betwork where it is not possible, or in any case economically disadvantageous, to implement it in wired form.
- **High throughput connectivity for companies and individual users**: satellite access is a winning solution in areas where terrestrial networks are unable to guarantee a certain quality of service in terms of bandwidth.
- **Connectivity in remote areas**: unlike the previous case, in those areas of the World that are not fully served by terrestrial networks, satellite technology represents the only possible solution to the problem (reduction of the Digital Divide).

- **IoT (Internet of Things)**: future satellite systems will have to be able to manage the traffic generated by IoT applications such as sensor networks, intelligent home automation systems, smart city systems and others.
- **Support to/integration with cellular networks**: backhaul connections for base stations unreachable by terrestrial networks and integration with latest generation cellular systems (Beyond-5G and 6G).
- **HDTV broadcasting**: ensuring High Definition Digital TV with interactive content for fixed and mobile users.
- **Multimedia contents**: management of traffic linked to data, audio and video content in digital format and generated by applications oriented towards online services, teleworking, telemedicine, e-learning, e-commerce and so on.
- **Telephony**: guarantee mobile telephone services in areas of the World not served by the traditional cellular network.
- **Mobile services**: guarantee secure and reliable connections to mobile end users, such as aircraft for PPDR (Public Protection & Disaster Relief), trains, ships, land vehicles and so on.

1.2 Satellite System architecture

Generally speaking a radiofrequency (RF) satellite communication system is constituted by three mains parts [1], called segments, as shown in Fig 1.1:

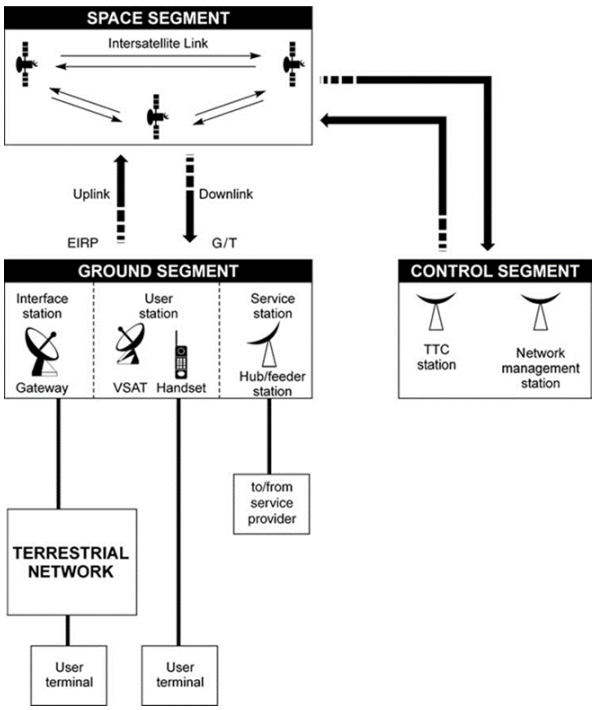

Figure 1.1: Satellite System architecture

- **Space Segment**: it consists of a single satellite or an entire constellation of satellites. Each satellite is in turn made up of a payload (P/L) and the platform (P/F) that hosts it. The P/L contains transmitting (Tx) and receiving (Rx) antennas and all those electronic systems responsible for transmitting and receiving carriers. In this context, the term transponder indicates the set of devices that are crossed by each of the N radio frequency (RF) channels from the Rx to the Tx antenna of the satellite; it follows that a single P/L can contain an N number of transponders. In fact, in the simplest case, the satellite performs the function of a multi-channel repeater carrying out filtering, amplification, switching, multiplexing and frequency translation, while in other more complex cases it can also carry out the routing of the carriers from an upbeam towards a given downbeam. The most complex case foresees a real on-board processing of the signal, after demodulation of the the uplink carriers. The P/F, on the other hand, includes all those subsystems that allow the correct operations of the P/L, such as propulsion, electrical power supply, temperature control, attitude control and stabilization, etc.
- **Ground Segment**: it includes all the ground stations that can be connected to the final end-user either through the already existing terrestrial communication network or directly connected to them in the case of small stations, called VSAT (Very Small Aperture Terminal). Ground stations can be divided into three types: final end-user stations, such as portable telephones, mobile stations and VSAT, which allow the customer to direct access the space segment; interface stations, known as gateways, which connect the space segment to the terrestrial network; finally service stations, such as hubs or feeder stations, which collect or distribute information from/to to user stations across the space segment. A peculiar aspect of ground stations is the size of the antennas, which can vary from a minimum of 0.6 m to a maximum of 30 m in diameter, depending on the volume and type of traffic that must be managed. Furthermore, stations can be Tx/Rx or Rx only.
- **Control Segment**: it consists of all the ground systems for controlling and monitoring the satellites and for managing the traffic and associated resources on board the satellite. Among them, the TT&C (Telemetry, Tracking and Command) system and the OBDH (On-Board Data Handling) system can be mentioned. The TTC system manages the operations of the entire spacecraft, by receiving control signals from the ground to carry out maneuvers and changes in the state and operating mode of the equipment, by transmitting the results of measurements and information about the operation of the satellite equipment, by verifying the execution of commands from the ground station, by allowing measurements of the distance between the satellite and the ground and its radial velocity in order to allow the localization of the satellite.

The ODBH system, on the other hand, manages all the processing and formatting operation of the service data together with the traffic data.

1.3 SATCOM payload achitectures

As introduced before, in a SATCOM mission the payload includes all those systems and equipment responsible for receiving, processing and transmitting signals. The architecture of a SATCOM payload can be more or less complex depending on the implemented functionalities. Generally in literature it is useful to divide SATCOM payloads into three large categories [2]:

- The simplest architecture is the so-called **bentpipe payload** (Fig. 1.2), which simply converts the uplink signal from one frequency to another one and then transmits it in downlink, in order to decouple the two paths (Rx and Tx) avoiding mutual interference between them. The received waveform is not demodulated, so that the received signal is not processed at the binary information level. For this reason, channeling (i.e. the operation of dividing the received band into the various channels and sub-channels) and routing can only be carried out at transponder level using analogue techniques and components. A first possible approach is the so called transponder-hopping, in which a pre-established frequency band Bij is assigned to all those users in the beam i that want to communicate with those in the beam j. A second approach, necessary when the number of beams to be managed becomes high, is the satellite-switched time-division multiple-access (SS/TDMA), in which time is divided into frames in such a way that the time Tij is used by all those users in the beam i and that want to communicate with the users in in beam j. Switching is carried out by a control unit that manages the connections between uplink and downlink, in a timed manner, with a switching matrix. The limits of this type of architecture consist in a heavy payload and high power consumption due to the use of analog solutions, an inefficient exploitation of the capacity offered by the individual transponders and in the fact that the effects of the corruption and degradation of the signal arriving in the uplink are inevitably transferred to the downlink signal.

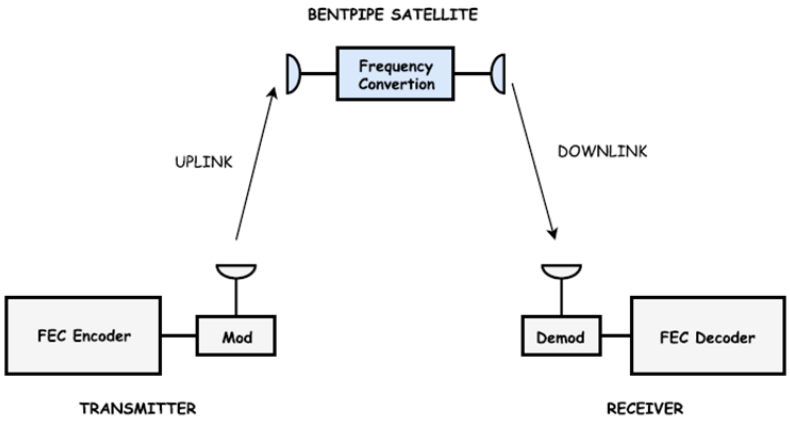

Figure 1.2: Bentpipe payload

- The most complex architecture is that of the **full-processing payload** (Fig. 1.2), in which the received signal is demodulated and decoded at the binary information level in order to regenerate the original signal and the related transmitted data. Once this is done, a recoding of the information and a remodulation of the signal is carried out before transmitting it again in the downlink, using modulation and coding schemes that are the same or different from those used in the uplink. The advantages of this approach are multiple. Routing can be carried out at the packet level so that the routing subsystem can be implemented using analog and digital components, allowing savings in terms of mass and power consumption and raching the optimization of the the bandwidth efficiency and the obtained throughput of the system. Finally, performance is also clearly improved in terms of achievable BER: since the signal is regenerated, its inevitable degradation in the uplink no longer affects its quality in the downlink. Obviously a payload of this type has the disadvantage of having a very complex functional architecture.

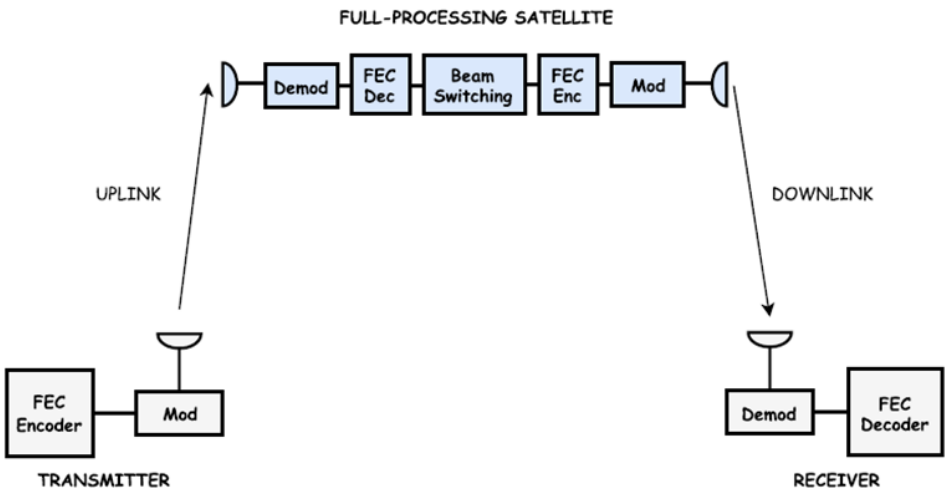

Figure 1.3: Full-processing payload

- A compromise between the two previously introduced architectures is represented by the **partial-processing payload** (Fig. 1.4). In a payload of this type the input uplink signal is demodulated but not decoded (a dual consideration can be made for the output downlink signal). For this reason, in case of corruption of the original binary information, it cannot be restored, in the sense that an error that occurs during the detection phase cannot be corrected. Anway, due to the presence of demodulation and modulation operations, the decoupling between uplink and downlink with regards to signal degradation due to radio channel impaiments and noise is still guaranteed. Due to the lack of decoding and encoding functionalities, packet routing is generally not possible: it can only be implemented if the packet header, which contains the routing information, is not encoded. In this case the overall packet is composed by the combination of an unencoded packet header and an encoded packet payload. Another possible approach could be to include in the payload architecture a full-processing subsystem that processes only the packet headers, which therefore in this case can be encoded. Taking in account all these considerations, it can be said that, as regards the end-to-end performance inherent to BER, a partial-processing payload has intermediate characteristics compared to the other two previous types of payload.

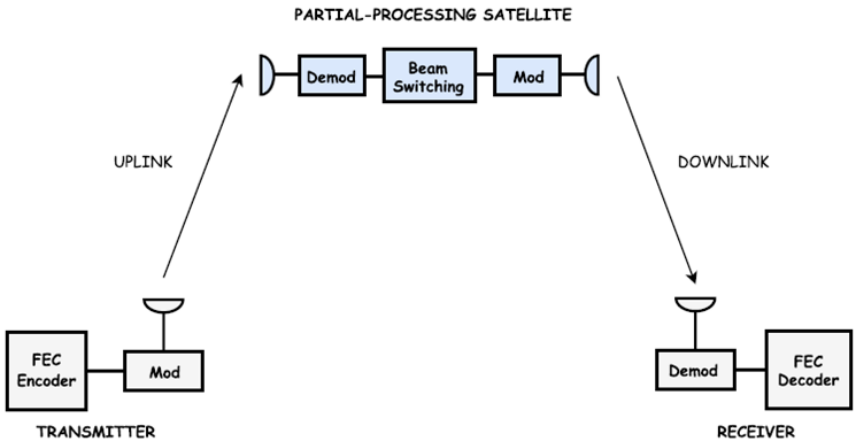

Figure 1.4: Partial-processing payload

1.4 Orbits taxonomy

The trajectory followed by the satellite during its motion around the Earth, in accordance with Kepler's laws, lies on a plane and generally has the shape of an ellipse, with the Earth occupying one of the its two foci, with the maximum extension at apogee and minimum at perigee. Furthermore, as a consequence of the principle of conservation of angular momentum, the satellite moves along its orbit more slowly when its distance from the Earth is greater, so that its orbital speed is, in module,

maximum at perigee and minimum at apogee. In relation to the most advantageous orbits in the SATCOM context, the main types of satellites can be classified as follows:

- **Low circular orbits** (LEO, Low Earth Orbit): the altitude of a satellite in this type of orbit is constant and equal to several hundred km, with an inclination close to 90° and an orbital period of the order of 1.5 h. This type of orbit ensures long-term worldwide coverage as a result of the combined motion of the satellite and the Earth's rotation. A constellation of several dozen satellites in low circular orbit (these satellites, having a speed of revolution around the Earth greater than its rotation speed and therefore a limited visibility time, must be in large numbers to ensure continuous coverage) can guarantee real-time communications (contained propagation delay of approximately 20-25 ms) with worldwide coverage. Currently these lower orbits are also exploited for a particular type of satellite system, that of the so-called "miniaturized satellites", i.e. satellites of reduced size and mass, such as mini satellites (from 200 to 400 kg) and micro satellites. (from 60 to 200 kg), just to give few examples.
- **Medium-height circular orbits** (MEO, Medium Earth Orbit): they have an average height of about 10,000 km, an inclination of about 50° and an orbital period of about 6 hours. In this case a constellation of approximately 10-15 satellites is able to guarantee continuous coverage of the Earth's surface.
- **Circular orbits with zero inclination**, i.e. equatorial orbits (GEO, Geostationary Earth Orbit): the best known is the geostationary satellite orbit, along which the satellite orbits around the Earth in the equatorial plane and in its own direction of rotation at a height of 35,786 km and with an orbital period of 24 h. For this reason, to an observer placed on the Earth's surface, the satellite appears as a fixed point in the sky. In this case, only 3-4 satellites are needed to guarantee global coverage of the planet, as each satellite continuously subtends an area of visibility equal to approximately 43% of the Earth's surface.
- **Elliptical orbits** on a plane inclined at 64° with respect to the equatorial plane: this type of orbit is particularly stable with respect to the irregularities of the Earth's gravitational field and, thanks to its inclination, allows the satellite to cover regions at high latitudes for large fractions of the orbital period when it passes through apogee. Continuous coverage can thus be obtained with three satellites appropriately phased in different orbits.

It should also be noted that it is possible to have hybrid satellite systems, which can include combinations of satellites on both circular and elliptical orbits. Obviously the choice of the most appropriate orbits depends on a series of considerations which may be the nature of the mission, the

extension and latitude of the area that must be covered, the elevation angle at which the satellite must be seen, the acceptable levels of interference and delay (e.g. considering time-tolerant and time-sensitive missions and services), the type of launchers to be used.

1.5 Current scenarios and future trends for SATCOM systems

As already hilighted at the beginning of this chapter, the space, and SATCOM in paricular, is experiencing an epochal renewal that is leading it to rapidly change its paradigm of "niche" technology to become something much closer to the common sense of consumer-type products and services as it is already in the case of mobile telephony, access to the Internet and so on. New satellite and contellation paradigms are catching on, providing wider services and opportunities.

A first notably example is provided by **High Throughput** and **Very High Throughput Satellite systems** (HTS and VHTS systems). They are advanced SATCOM systems, mainly in Geostationary Orbit (GEO) but also in Non-Geosstationary Orbit (NGSO), capable to provide significantly higher data transmission capacity (hundreds of Gbps) with respect to to traditional satellites (tens of Gbps) and supporting a wide range of services like broadband internet, cellular backhaul, government/military communication, and in-flight connectivity, ensuring at the same time a lower cost per transmitted bit compared to traditional satellites. This is possible due to the fact that these kind of systems are capable to ensure an optimized service, dinamically tuned on the bais of the user's needs in therm of traffic, coverage, Quality of Service (QoS) and so on, for example by implementing flexible ground coverages (i.e. the cability to provide a dynamic adaptation of the coverage during the flight and/or the generation of new coverage areas) and flexilbe management of on-board resources (e.g. the possibility to adjust dinamically the power per channel in order to follow communication needs or to face with communication impaiments, the possibility to change over time the number of available channels on a specific coverage area, the possibility to dinamically coordinate the frequency plan according to traffic and coverage variations). These capabilities rely on the implementation of innovative technological approaches [3-4]: higher frequency bands, such as Ka, Q/V and W, narrow multi-beam ground coverages (from tens to hundreds of spot-beams), frequency reuse, advanced On-Board Processing (OBP) capabilities (e.g. with signal regeneration).

The second example of new satellite constellation paradigm is provided by **mega-constellation**, a group of satellites tipically in Low Earth Orbit (LEO), i.e. altitude < 2000 km, operating together to cover a huge part, or eventually the whole totality, of the Earth surface. These satellites are placed on a surface defined by various orbits near to each other and connected to form a space network, i.e. a network of satellites in which each space node is able to be connected to some others by means of

Inter-Satellite-Links (ISLs) and Inter-Orbit-Links (IOLs), in addition to the connectivity with the Ground Stations (GS) by means of feeder links (FLs). In the field of mega-constellations, three important players are OneWeb [5], SpaceX with the Starlink constellation [6], Telesat with the Telesat Lightspeed constellation [7] and finally Amazon with the Kuiper project [8]: a technical comparison of the above space systems, especially in terms of total throughput and number of served gateway antennas on ground, is provided in [9]. Mega-constellation satellites can rely on improved capabilities due to digital payloads implementation, steerable multi-beam antennas implementing frequency reuse schemas (in the same way of the terrestrial cellular networks), high performance modulation and coding (MODCOD) techniques, etc. Other key features and technologies are analyzed in [10]. Finally, the main opportunities guaranteed by mega-constellations [11] are the provision of broadband communication over a fair and global coverage and the capability to support delay-intolerant applications requiring a reduced latency, e.g. 250-350 ms of round-trip-time (RTT) of a GEO satellite versus 30 ms of RTT for a LEO one.

The third example is provided by the concept of **Space Optical Transport Network** (Space OTN) [12-14], a satellite constellation composed by a certain number of space nodes (in GEO, MEO and LEO orbits) with the capability to establish space-space and space-ground links in the optical frequencies instead of the radiofrequency (RF) ones. Compared with the RF links, the Free Space Optical (FSO) links present some advantages such as higher achievable data rates, smaller antenna sizes (leading to reduced on-board mass, volume and power consumption), higher directivity and lower beam divergence, leading to higher resilience to interference and higher security (no possibility to intercept or jam the optical beam), no constraints coming from spectrum allocation regulation [15]. A comprehensive summary on technologies and applications of FSO links to satellite communication networks is provided in [16]. An innovative space system concept is represented by the European Data Relay System (EDRS), a European constellation currently composed by two GEO satellites (EDRS-A launched in January 2016) designed to provide data relay and data forward services based on both optical and RF (Ka band) Inter Satellite Links (ISLs) with non-geostationary satellites, space-crafts, Unmanned Aerial Vehicles (UAVs) and classical RF connectivity with Earth stations [17-19]. In addition to the FSO links, as in the case of the EDRS system but also applicable to small satellite constellations as above [20-22], allowing in line of principle connectivity between space nodes (implementing some network topologies such as ring or mesh) and with the optical stations on ground (if Optical FL is present), a further improvement to the system is provided by the implementation of on-board wavelength circuit switching: if Wavelength Division Multiplexing (WDM) is adopted, space nodes with routing/switching capabilities can implement optical circuit switching by

demultiplexing optical channels at each input port, routing each of them independently to the required output ports and finally multiplexing again all the wavelength at each output port [23]. Such as space infrastructure can integrate the transport service provided by the terrestrial network in a vision of seamless integration between the Space OTN and the Ground one.

Another promising space network scenario is represented by **micro and nano satellite constellations**, in particular cubesats [24]. Considering their reduced dimensions and limited costs for development and launch, cubesats can be exploited for a wide range of missions and applications such as technology demonstration, Earth observation, communication, deep space exploration, educational and scientific purposes, surveillance [25-26].

1.6 The new concept to conceive and implement SATCOM

The representative scenarios described in the previous paragraph constitute the starting points to conceive a new concept of SATCOM system implementing, as already done in the terrestrial case, a full networking capability in the satellite telecommunication infrastructures, as depicted in Fig. 1.5.

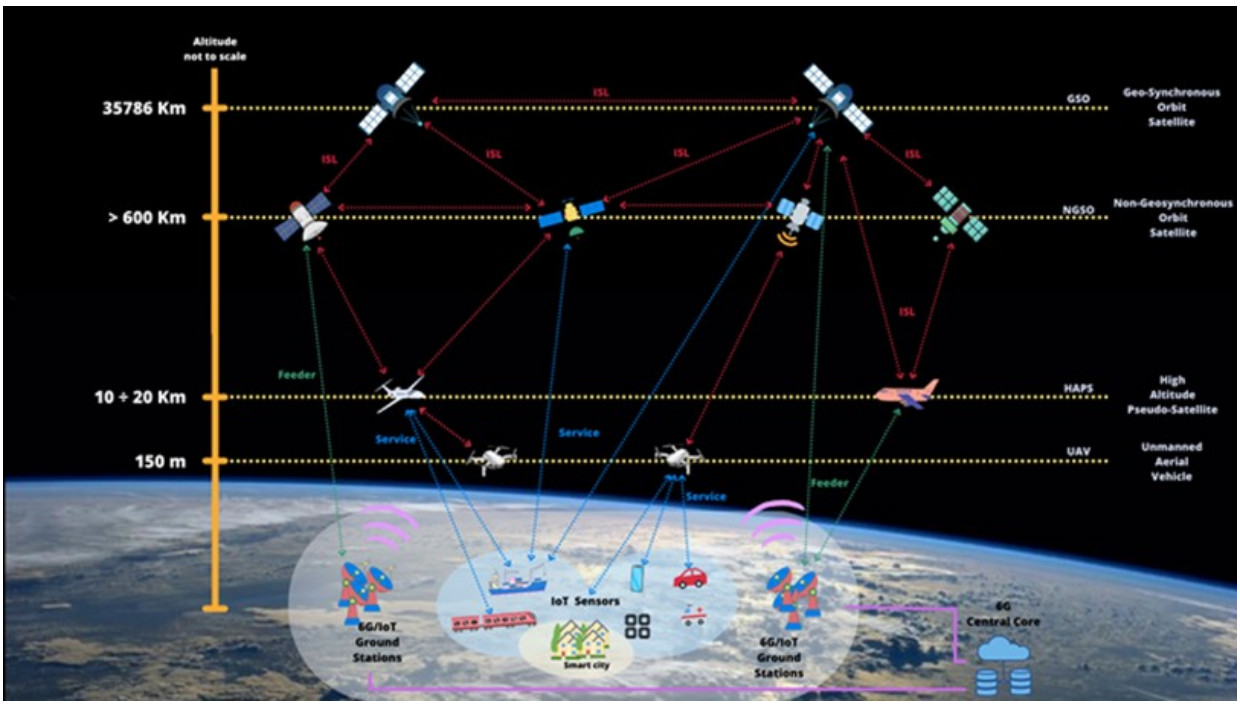

Figure 1.5: Architecture of an heterogeneous integrated space-terrestrial network

The two main pillars on which this architecture is based are:

- **Heterogeneity**, due to the fact that such a network interconnects different typologies of nodes, i.e. space nodes (satellites at different altitudes), airborne nodes (e.g. airplanes, UAVs, high altitudes balloons, drones, …) and terrestrial/maritime nodes (both fixed and mobile);

- **Integration**, since different kinds of networks are seamless interconnected each other, being transparent from the user service and experience point of view.

Such a network has a tree-dimensional architecture composed by different layers. Satellites at different altitudes (GEO/MEO/LEO-VLEO) constitute the more external layers. The interconnections between themselves (by means of ISLs-IOLs) and with stations on ground (by means of FLs) represent a backbone network in space providing transport/trunking services, e.g. delivery of high amount of aggregated traffic: in the specific case GEO links are suitable for delay tolerant traffic, LEO more suitable for delay sensitive traffic. In addition, they can also provide access to users in space (e.g. other satellites without FL capability, airborne users, …) and on ground (e.g. ships, ground users in remote locations not served by terrestrial connectivity, …). Airborne nodes are both inter-connected to space and potentially also with ground. Finally ground nodes (in addition to maritime ones) are part of terrestrial networks such as cellular mobile networks (user mobiles connected to the relevant Base Tranceiver Stations), satellite ground stations (GSs) connected to internet, mobile satellite terminals, sensor networks for IoT Applications, etc. It is worth to note that this kind of scenario requires the capability to interoperate different pieces of network relying on different physical media and protocols.

2. Photonic technologies for SATCOM systems

All the current future scenarions described at the end of the previous chapter are supported by a wide range of technologies that, originally developed for terrestrial applications, currently are being integrated in space applications. For example, Beyond-5G and 6G technologies give an opportunity for the integration of Non-Terrestrial-Networks (NTNs), which include LEO-VLEO satellite constellations [27], into already existing terrestrial infrastructures, with the aim to create an integrated seam-less hybrid network [28]. In this sense the Third Generation Partnership Project (3GPP) has defined a set of architectural scenarios to enable 5G protocol to support NTN networks [29-30]. Also Internet of Things (IoT) applications [31] can take benefits from support provided by satellite communication systems. In addition to the abovementioned technologies, mainly solving the issue to interoperate different networks relying on different protocols, optical/photonic technology represents the key enabling solution to overcome the inherent technological problems relted to such a complex systems, as emerged in [32-34], in addition to their the high-demanding data rate target (terabits communication as final future goal), and it has been extensively studied [35-37]. Otical/photonic technology can be successfully exploited mainly at two levels:

- **Payload level**, by making more efficient and simple on-board payload functionalities and operations usually perfomed if the electical/microwave domain;
- **Link level** (space-space and space-ground), by providing an alternative to classical RF links with an increased performace in terms of achievable capacity and without regulatory constrains and "frequeny oppression issues" as in the RF case.

Anyway it is worth to note that the optical/photonic technology does not provide a fully alternative to completely replace the standard microwave one due to the following reasons [38]:

- In current SATCOM systems the User Segment is implemented in standard RF/electrical technology, with a high degree of technological maturity at reduced costs; the user-side terminals exploit RF links to have access to the Space Segment and sometimes these same terminals can also be shared to have access to terrestrial networks, as in the case of cellular telephony. All this makes optical link technology inapplicable and inconvenient on the User Segment side and this translates, at payload level, into the impossibility of completely renouncing to the presence of RF sections (e.g. antenna systems in Tx and Rx, initial RF filtering and amplification operations, etc.). Instead optical links can be effectively implemented in case of gateways (OGSs, Optical Ground Stations) owned by SATCOM

Operators handling aggredated traffic (i.e. trunking service), corporate ground stations or OGSs for military scopes, thus justifing the had-hoc applications and related costs.

- It is more convenient to consider photonic technology as a solution to be integrated with RF technology, rather than a total replacement of it, due to the technological advantages provided by the current state of advancements of RF technology, which has been obtained thanks to the investments made over time by various players in the space technology market (primarily Satellite Operators). So the most convenient and gradual way to introduce photonics in the SATCOM context is to propose the replacement of payload subsystems/critical units for which RF technology has achieved significant improvements or is too complex to implement with respect to the photonic equiovalent ones. In addition, while photonic technology is fully mature for terrestrial applications, some architecture and implementations need to br qualified for space applications.
- The coexistence of both photonic and microwave technologies is the best way to carry out a performance comparison between them, in order to demonstrate to Satellite Operators and in general to all customers in the space market the achievable improvements in terms of size, weight, power consumption and, in perspective, cost savings.

2.1 Benefits of combined micrewave-photonic technologies

As a consequence of the increase in target perfomances and in payload architecture complexity foreseen for the SATCOM scenarios prevously introduced, a proportional growth in on-board needed resources (in terms of mass budget, power budget, numbers of equipment to be embarked, etc.), and consequently in costs, is expected. By way of example, in the futuristic VHTS scenario described in [39] with a payload providing 1008 spotbeams on the user side and 90 spotbeams on the gateway side, the payload budgt shows a mass of 3989 kg and a power consumption of 58, 8 kW; the power dissipation corresponds to 43,5 kW, correspong to a power efficiency of only 26%. In addition to the above described issues, an increased payload complexity brings also the increase in the duration and complexity of the assembly, integration, test and verification phases (AIT-AIV, Assembly Integration Test and Verification) must also be taken into account, as well as the costs related to the launch. To face with these problems, the introduction of photonic technology for the implementation of some functionalities within a SATCOM payload can bring to potential advantages if compared with their implementation in the traditional RF/microwave technology [40]:

- Reduction of the number of on-board equipments and components bringing to mass and volume saving, thanks to the intrinsic characteristic of photonic technology to be miniaturised;

- Reduction of the required power budget (this aspect, anyway, will be more significative only with a complete payload implementation in photonic technology);
- Improved performance in terms of bitrate/bandwidth;
- Reduction/immunity from electromagnetic interference (EMI);
- System transparency, i.e. independence of input/output from the frequency of the RF signal;
- Low payload internal propagation losses;
- Reduced risks during the launch phase (robustness against vibrations, electromagnetic compatibility, etc.);
- Easy scalability of functionalities to be implemented, e.g. scalability of switching/routing functionality on large payloads where current standard microwave technologies may be unfeasible.

A direct consequence of the above mentioned advantages consists in the reduction of the total costs for launching satellite systems guaranteeing a given processing and transmission capacity (Cost for In-Orbit Delivery of Capacity): for this reason photonic technology can be exploited with advantage in a series of future mission scenarios ranging from the already introduced Terabit systems (VHTS) to mega-constellations of LEO/MEO satellites, to different applications such as Navigation, Earth Observation and Deep-Space exploration. Another consequence is the reduction of the costs related to payload manufacturing [41] due to different aspects such as reduction of all analytical and testing activities related EMC compatibility verification and certification, reduction of engineering effort for payload accomodation (faster unit installation and test on spacecraft panels due to a reduced payload complexity) and so on.

2.2 Benefits of free space optical communication

Satellite-based Free Space Optical (FSO) communications represent a cutting-edge technology providing an alternative approach, if compared with classical radiofrequency (RF) communications, to transmit data across free space. It cannot be considered a fully replacement for the RF one due to the fact that FSO links allow only a point-to-point connectivity and also considering that RF systems represent a consolidated and proven solution for SATCOM missions. The Table 2.1 below provides a summary on the comparison of these two technologies across various aspects:

Table 2.1: Comparison between RF and FSO technologies

FEATURE	RF TECHNOLOGY	FSO TECHNOLOGY
Licensing	Limited and shared by multiple users.	License-free operations.

FEATURE	RF TECHNOLOGY	FSO TECHNOLOGY
Bandwidth	Higher available bandwidth capable to support datarates in the order og gbps or higher.	Lower available bandwidth.
Security	High resistance to eavesdropping and jamming.	Possibility to intercept or block the communication.
Interference	Immunity to electromagnetic interference.	Lower robustness to interferring signals and other noise sources.
Alignment	Line-of-sight not required.	Line-of-sight required.
Divergence	Higher beam divergence due to the higher operative wavelenght range.	Reduced beam divergence, translating into the capability to supply the same power density in a longer distance, given the Tx antenna dimensions.
Pointing requirements	Less constrained pointing requirements due to higher beam divergence.	Demanding pointing requirements, translating into remarkable losses due to pointing error.
Environmental conditions	Less affected by atmospheric conditions	Strong dependance from atmospheric absorption, scattering, turbulence, rain, fog, snow, pollution, etc.

In conclusion, both FSO and RF communications have their advantages and limitations. Certainly FSO offers higher bandwidth, faster data transfer speeds and enhanced security, anyway the choice between them depends on the specific requirements of the application, environmental factors and available technology.

2.3 Hybrid microwave/photonic payload concept for RF-based SATCOM

As investigated in some activity studies conducted by the Europen Space Agency [42-43] and the European Commission [44], the introduction of photonic technology in SATCOM systems, based on RF links, is achievable by means of the definition of a hybrid microwave/photonic payload architecture in which a set of payload functionalities, and the related subsystems, can be implemented

in the optical domain instead of in the electrical one [45]. In detail the main functional building blocks to be considered for implementing on-board functionalities in the optical domain are [34,40,42,43]:

- **Photonic frequency generation** provides the satellite with the needed reference RF frequencies by directly generating them in the optical domain and subsequently distributing them in the same way (photonic local oscillators and optical amplifier are needed);
- **Photonic frequency conversion**, for the mixing in the optical domain of received RF signals in order to perform up/down conversions (electro-optical mixers and opto-electronic detectors are needed);
- **Photonic routing/switching and on-board subsystems interconnection**, providing the optical signal routing capability (large optical switching matrix) and the interconnectivity to all the hosted photonic components (optical couplers and switches, power combiner/divider, WDM multiplexer/demultiplexer, optical filters, fibres and connectors are needed).
- **Photonic beamforming**, which provides the capability to control the directivity of electromagnetic waves using optical components: instead of using electronic devices, in photonic beamforming incoming electrical signals are converted into optical ones; after being manipulated to give them the required phase shifts, they are converted again in the electrical domain to feed the antenna elements.

All the abovementioned building-blocks are supported by a set of "basic operations" implemented in the optical domain providing a functional architecture of the telecommunication payload, as described in following.

Electro-optic (EO) and Optical-electric (OE) conversion

On the basis of the frequency range of the RF signal to be translated in the optical domain, two approaches can be applied for EO conversion: i) direct modulation of the laser diode for low frequency RF signals (e.g. 5-10 GHz) not exceeding the electrical band-width modulation of the laser source and ii) externally modulated laser diode, recurring to an electro-optical modulator (e.g. LiNbO3 modulators) for higher frequency ranges (e.g. more than 10 GHz). It is worth pointing out that for OE conversion, photodiodes with high bandwidth detectable signal and good responsivity are available (e.g. pin InGaAs photo-diodes at 1550 nm).

Reference frequency generation

A set of RF reference signals are produced and then transferred on different optical carriers, constituting the on-board photonic local oscillators which are involved in further signal processing functionalities such as frequency up-down conversions. For this purpose, two different approaches are possible. The first approach is derived from the abovementioned EO conversion techniques, implying conventional RF/microwave oscillators. The oscillator signals are transferred over optical carriers by means of direct modulation or external modulation of a continu-ous wave laser. This latter solution offers the advantage of exploiting the intrinsic non-linearity of Mach-Zehnder electro-optical modulators and their different bias point (QB, i.e. Quadrature Bias point or MITB, i.e. Minimum Transmission Bias point). There-fore, it is possible to obtain harmonics of the input reference frequency and to achieve the final generation of 100 % modulation high spectral-purity oscillators up to 30 GHz. The second approach is suitable for the generation of reference oscillators in very high frequency bands, e.g. Q/V bands, with high spectral purity and stability. It consists in generating these signals directly in the optical domain exploiting free space cavity-based optical oscillators, fibre-based optical oscillators, optoelectronic oscillators and electrooptical modulator based optical oscillators.

Filtering of RF signals in the optical domain

Microwave photonic filters offer some advantages with respect to the conventional technology, e.g. high bandwidth availability (up to THz frequencies), tunability and re-configurability, reduced mass and volume. A typical configuration is the discrete time delay-based one [46].

Optical routing/switching

In the optical domain, the capability to perform on-board switching operation is nec-essary to manage the connectivity between different spot-beams both in the up-link and in the down-link. For optical switching implementation, different technologies can be considered [47] such as thermo-optical switch, electro-optic switch (based on LiNbO3), Semi-conductor Optical Amplifier (SOA) based switch and Micro-Opto-Electro-Mechanical System (MOEMS) based switch [48].

Optical distribution of signals and optical amplification

The implementation of payload subsystems interconnection exploiting the photonic technology (by means of optical fibres, mux/demux, coupler/divider, etc.) has the main advantage of allowing the replacement of traditional microwave/electronic interconnections such as copper cables, coaxial cables, microwave waveguides, etc. Traditional interconnections are suitable only for the particular

frequency range for which they are designed. Conversely, optical fibres can be exploited to transport over optical carriers RF signals in any frequency range, following the same approach of the terrestrial RoF (Radio over Fiber) technique and leading also to a mass and volume saving. Optical amplifiers, such as Erbium-Doped Fibre Amplifiers (EDFA) and SOA, can be exploited to recover interconnection optical losses.

Photonic mixing for RF signal up/down conversion

The RF signal frequency conversion, e.g. obtained by means of intensity LiNbO3 Mach-Zehnder modulators used as electro-optical mixers, is the operation performed in the optical domain achieving most advantage. Actually it ensures: i) high isolation between the modulator port, to which the local oscillator signal is applied, and the one to which the RF signal to be up/down converted is applied; ii) large achievable electrical bandwidth (in the order of hundreds of GHz); iii) single-step frequency conversion in high frequency ranges for which usually more than one mixing stages are needed in the conventional electronic technology; iv) multiple and simultaneous frequency conversions exploiting a WDM (Wavelength Division Multiplexing) approach. Considering for example the case of the down conversion (but the same considerations are valid for the up conversion), this last technique makes available at the same time a set of different intermediate frequency f_{IF} signals coming from the same input RF f_{RF} signal by mixing them with different photonic local oscillators. Each local oscillator is transported over a different optical channel belonging to the WDM wavelengths set. In the same way, it is possible to down convert simultaneously a set of different RF signals, transported over different WDM channels, by mixing them with a photonic local oscillator.

Fig. 2.1 shows the concept of a microwave/photonic based SATCOM payload, in which the basic operations of the architectures described above are implemented.

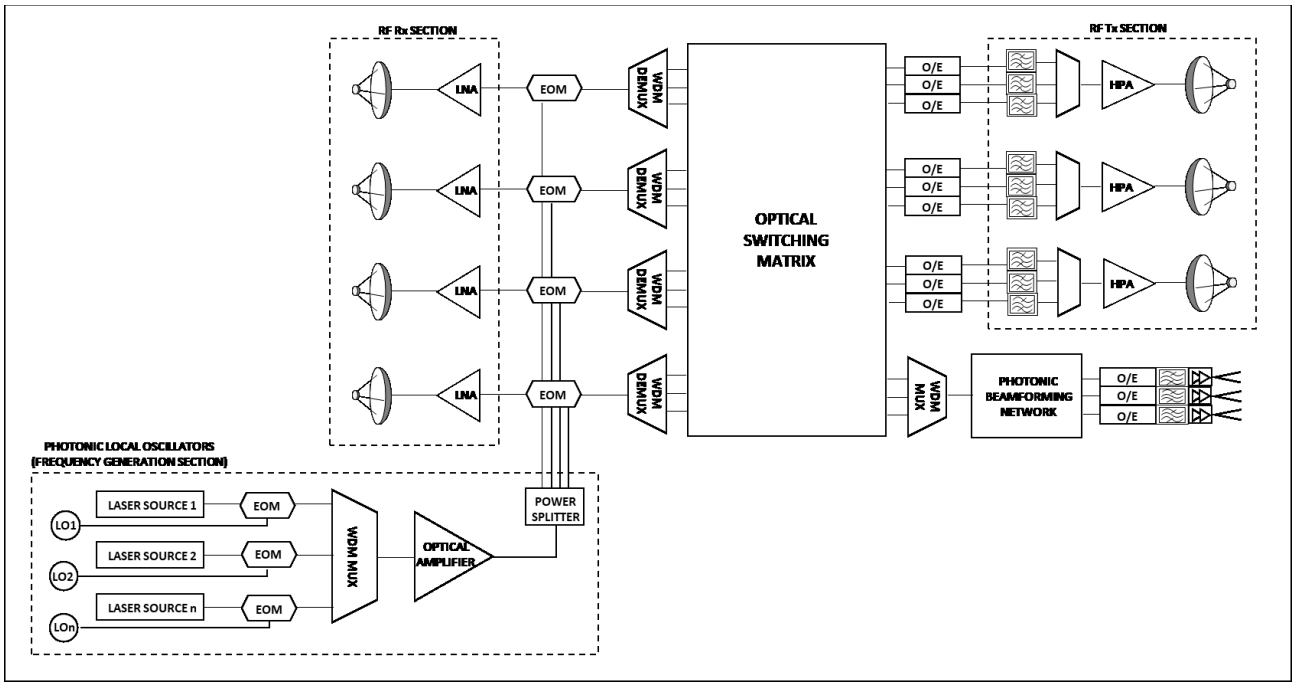

Figure 2.1: Microwave/Photonic SATCOM payload concept

The photonic frequency generation section, containing the reference frequencies of all the local oscillators, feeds simultaneously all the electro-optical modulators. The signals coming from the receiving RF front-end (i.e. the signals that, after the Rx antennas, have been filtered and low-noise amplified) are translated in the optical domain and frequency converted. After that, the optical channels are separated by means of WDM demultiplexers and routed separately by the optical switching matrix (e.g. according to the requested connectivity in a multi spot beam coverage scenario). Finally, at the output ports of the optical switch, each optical channel is converted again in the electrical domain before reaching the RF transmitting section.

2.4 Optical payload concepts for FSO-based SATCOM

As already introduced in the previous chapter, in parallel to the definition of RF-based SATCOM systems supported by photonic technology, the research effort of the institutions, with the support of industries and academic entities, is aiming at the definition of satellite telecommunications systems based on free-space optical links, namely FSO satellite communications. This is the emblematic case of the HydRON (High-thRoughput Optical Network) Project, started in 2024 with the lead of ESA and supported by the main European space players, aimed to to build a network of high-capacity optical inter-satellite links and ground-satellite links that interconnect space assets each other and with ground networks and that seamlessly extends the terrestrial optical transport networks into space, according to a “fibre-in-the-sky” vision [49]. This kind of application leads to the identification of additional optical payload architecures, since in this case not only the on-board signal elaboration in

the optical domain (fully or partially) it is implemented (as shown in the above payload architecural concept), but also the end-to-end connectivity with space and ground nodes. The underlying technology in this case is still represented by the WDM technique, in which different signals are assigned to different carriers, in order to exploit in a better way all the available bandwidth (e.g. in the case of Dense WDM (DWDM) carriers are so near, 100-50 GHz of carrier spacing, to accommodate a huge number of signals in the system. Several kinds of payload architecure can be conceived, as explinded in following:

Fully transparent optical payload

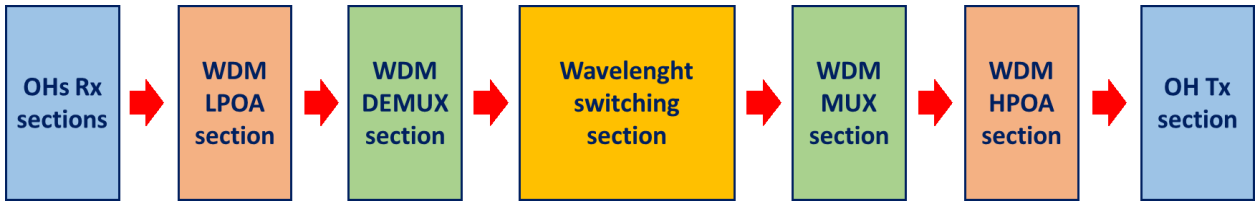

Figure 2.2: Functional block diagram of the fully transparent optical payload architecture

In this architectural configuration the signals processed and carried out remain in the optical domain from the input sections to the output sections of the payload. This implies that no electrical data regeneration is performed on-board (only optical amplification of the Rx WDM channels i.e. 1R signal regeneration) and the optical payload only performs in-space light paths set up and WDM channels routing. The main payload elements are:

- WDM transparent bidirectional (Tx and Rx) Optical Heads (OHs);
- Input/Output optical amplifier sections;
- Low Power Optical Amplifier (LPOA) section (i.e. the low noise pre-ampli- fier);
- High Power Optical Amplifier (HPOA) section (i.e. the booster amplifier);
- WDM channels DEMUX and MUX sections;
- Reconfigurable optical switching matrix (OXC or OADAM);
- Optical harness and fibres to interconnect payload subsystems.

In this case no on-board laser sources and receivers are foreseen to be hosted on the payload because the routed signals are only those received from incoming FSO links and forwarded towards out coming FSO links after being processed (essentially amplified and routed).

Transparent optical payload with OEO (Optical-Electrial-Optical) regeneration

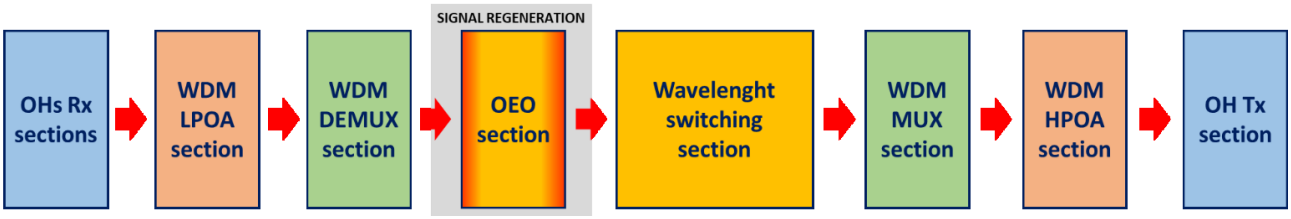

Figure 2.3: Functional block diagram of the transparent optical payload with OEO regeneration

This configuration is the same of the previous analysed, but an additional section of signal OEO regeneration (2R/3R) is considered in order to overcome the issue of the excessive degradation of the OSNR in a multi-hop link propagation and the consequent BER degradation experienced end-to-end. Typically an OEO signal 2R/3R regeneration foresees the exploitation of a non-linear element (e.g. a decision flip-flop) providing 2R regeneration (i.e. pulse re-shaping) with the addition of the clock recovery provideing 3R regeneration.

Optical payload with signal processing in the electrical domain

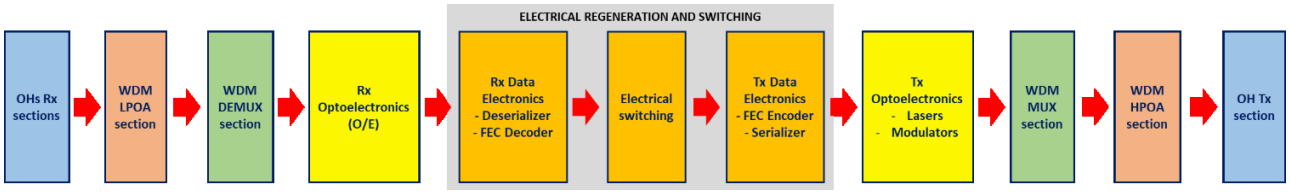

Figure 2.4: Functional block diagram of the optical payload with signal processing in the electrical domain

In this last configuration the implementation of the optical/photonic technology is limited only for the optical links: once the WDM channels have been demultiplexed, they are converted in the electrical domain in which they are processed (and so regenerated) and routed before being transmitted again optically.

2.5 Considerations on proposed payload concepts

In the two previous sections several concetpts of photonic-optical payload have been introduced, by describing their funcional architecture and the high-level operations performed on signals. It is clear that the main difference is in the field of applicability of optical and photonic technologies and techniques. In fact the first concept (hybrid microwave/photonic payload) proposes a typical telecommunication RF payload architecture in which photonic devices are exploited instead of their electronic/microwave counterparts: no architectural changes are foreseen neither before/after the payload Rx/Tx RF front-end (i.e. communication carriers are in the RF spectrum), nor in the termials on grund (on the feederlink and userlink sides). Instead the last three ones (optical payloads) rely on

a FSO communication concept, so that also payload Rx and Tx sections implement photonic means (i.e. communication carriers are in the optical wavelenght spectrum) as much as terminals on ground. Nevertheless the underlying technology is in common (laser sources and detectors, optical photonic modulators, optical isolators and filters, mux/demux elements, optical amplifiers, optical swithing matrices, optical fibres and connectors) even if implemented in different subsystems: for example photonic frequency convertes and beamformers are limited to the microwave/photonic payload, optical front-end (mainly OLPA/OLNA) only in the optical payload, optical swithing matrix potentially in common (depending on the chosen architecture).

Finally it is worth to note that the distinction in the different payload architectures as presented above is actually introduced to ease the disertation and system taxonomy. Anyway at mission level a mixed system is conceivable, considerig for instance a payload providing a multibeam RF coverage on the user side and a FSO link on the feeder side.

Moving from this context, the following chapters will focus on some of the subsystems included in the discussed payload architectures: for each of them, after a short technological state-of-the-art overview, a system simulation and performance evaluation will be provided.

3. Hybrid microwave/photonic multi-frequency up-down converter

Frequency up/down conversion is the first operation implemented on a SATCOM payload to be considered, in this thesis work, for implementation in the optical domain. In particular this chapter [50-51] will investigate a configuration of a microwave-photonic mixing stage used as down converter (but this in not limiting due to the fact that architecture is the same in case on up-conversion) based on a dual-port Mach-Zehnder Modulator (MZM) and a WDM configuration provided by two photonic local oscillators, at two different wavelenghts, used to demonstrate the simultaneous down-conversion of a given RF input signal into two lower frequency signals.

3.1 Technological state-of-the-art overview

In a SATCOM system tipically uplink signal frequencies are higher with respect to the downlink ones for two main reasons:

- Link performances are driven by Tx antenna's EIRP and Rx antenna's G/T. Since on-board resourcess in terms of volume, mass and power consumption are more constrained with respect to ground, an higher uplink frequency allows to achieve an acceptable gain for the on-board Rx antenna without requiring the respective increase of its dimension (wehile this is not a problem for antennas on ground, whose design is less constrained).
- Irrespective to on-board and on-ground antennas design, Free Space Path Loss (FSPL) is frequency dependant and it is more impacting for higher frequency signals with respect to lower ones. It follows that higher frequencies are assigned to the uplink since transimming power from ground is less constrained with respect that available to the satellite, where as already said on-board resources are tipically more limited.

As a consequence, frequency conversion represents a common operation perfomed on every SATCOM payload: if it acts only as a simple repeater, only the down-conversion of the received carriers is performed before retransimming them in downlink; if it has some kind of on-board processing capabilities (e.g. carrier demodulation/modulation, baseband signal manipultion, decoding/encoding, …) also up-conversion is required (e.g. from baseband) before downlink transmission. In any case these kind of operations are usually perfomed by electronic mixing stages. On the other hand the photonic implementation of this operation on RF signals brings some notably advantages [52]:

- No leakage of signals between the modulator ports (local oscillator port and RF signal port) ensured by their high isolation;
- Capability to process wide band signals (in the range of hundreads) of GHz and to perform single-step frequency conversions when typical electronic recnologies requre more than one mixing stage;
- General improoved performances due to low loss and immunity to electromagnetic interfererence (EMI).
- Possibility to obtain the simultaneous frequency conversion of a given signal into more than one translated signal by using the same mixing stage if WDM optical signals are implemented.

Several approaches and architectures have been identified to perform photonic-based microwave mixing for frequency conversion [53]. Since frequency conversion is due to a nonlinear process, it can be obtained exploiting two kinds of nonlinearities. i.e. all-optical and optoelectronic nonlinearities, as summarized in Figure 3.1.

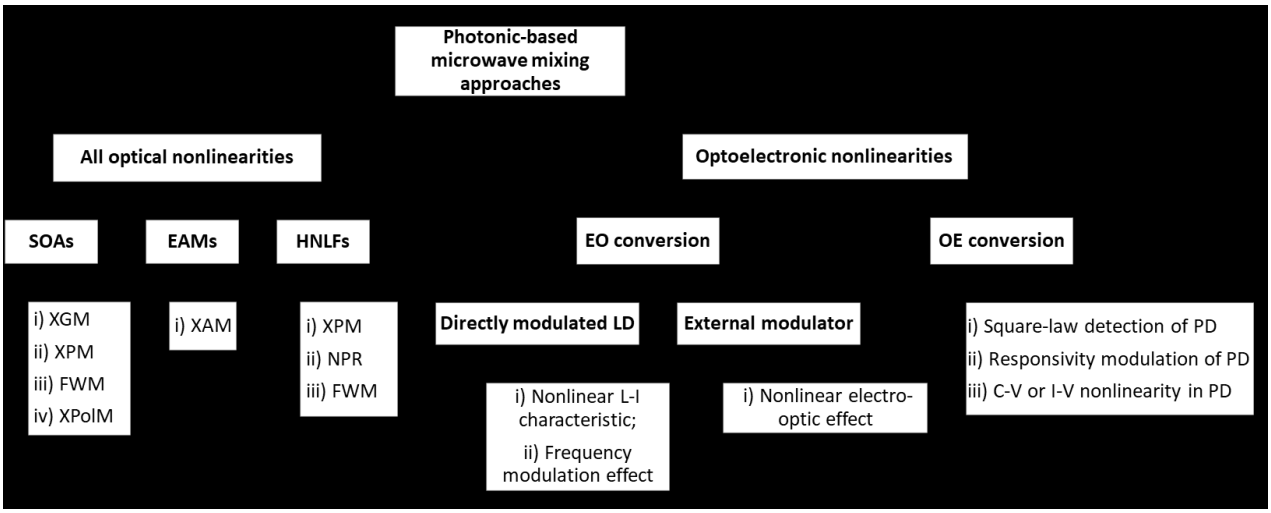

Figure 3.1: Photonic-based microwave mixing techniques [53] (SOA: Semiconductor Optical Amplifier; EAM: Electro Absorption Modulation; HNLF: Highly NonLinear Fibre; XGM: Cross-Gain Modulation; XPM: Cross-Phase Modulation; FWM: Four Wave Mixing; XPolM: Cross-Polarization Modulation; XAM: Cross-absorption modulation; NPR: Nonlinear Polarization Rotation; LD: Laser Diode; PD: photo-diode).

For what concerns all-optical nonlinearities, basically semiconductor optical devices and nonlinear optical fibers can be considered. In semiconductor optical amplifiers (SOAs), nonlinear effects such as cross-gain modulation (XGM), cross-phase modulation (XPM), four-wave mixing (FWM) and cross-polarization modulation (XPolM) are exploited to achieve RF frequency mixing. Cross-absorption modulation (XAM) is exploited in case of electro-absorption modulators (EAMs). For what concerns optical fibres, the third-order nonlinear effects such as XPM, nonlinear polarization rotation (NPR) and FWM are used especially in highly nonlinear fibers (HNLFs) to achieve frequency

mixing. For what concerns optoelectronic nonlinearities, since EO and OE conversions exhibit nonlinear behavior, microwave frequency mixing is achieved in case of EO conversion by i) directly modulated laser diodes (LDs) or ii) external modulators. The directly modulated LDs exploit the nonlinear light-current characteristic or the frequency modulation effect due to carrier density variation. In this case, FM-AM conversion is required and it is performed by an unbalanced MZI between the LD and the photo-diode (PD). In the case of external modulator usage, the nonlinear electro-optic effects are exploited. For what concerns OE conversion, the exploited mechanisms are: i) square-law detection of a PD fed by the optical RF signal and by the optical LO signal on the same optical carrier, ii) responsivity modulation of a PD fed by the optical RF signal and by the op-tical LO signal on two different optical carriers, iii) capacitance-voltage (C-V) or current-voltage (I-V) nonlinearity in a PD fed by the intensity-modulated optical RF signal and by coupling the electrical LO signal to the same PD.

In [54] further configurations for frequency conversion are described, foreseeing the usage of one or more optoelectronic mixers implemented by external modulators.

Then, starting from these architectures, other schemas have been furtherly identified to perform microwave-photonic frequency conversion: in [55] a mixer configuration based on an optical hybrid for down-conversion is described, where the selection of a given photodetection method (direct detection, balanced detection, double detection) allows to implement different mixing architectures, i.e. a single-ended photonic microwave mixer, balanced mixer, I/Q mixer or image-reject mixer (IRM). Authors in [56] present an ultra-wideband tunable frequency converter scheme for microwave and millimeter-wave signal generation based on optical recirculating loop and microwave-photonics technique (including dual parallel Mach-Zehnder modulator, optical filter and wideband photodiode), while those of [57] show a multi-band microwave signal down-conversion scheme based on optical frequency comb (OFC). In [58] the autors describe and experimentally implement a microwave photonic frequency conversion system based on a dual-loop optoelectronic oscillator (OEO): the dual-loop OEO generates the local oscillation (LO) signal and the up/down conversion states can be chosen by changing the bias voltages of the dual polarization dual-drive Mach-Zehnder modulator (DPDDMZM). In [59] the realization of a monolithically integrated InP photonic downconverter, based on dual parallel Mach-Zehnder modulators is achieved while in [60] the authors demonstrate the experimental implementation on the same silicon chip of two photonic mixer stages: the first based on a single dual-drive MZM and a single PD, the second one based on a dual parallel single-drive MZMs and balanced detection. Furthermore, additional architectures based on dual-drive Mach-Zehnder Modulator (DDMZM), polarization-division multi-plexing Mach-Zehnder Modulator

(PDM-MZM), cascaded phase modulation and optical filtering, dual-parallel Mach-Zehnder Modulator (DPMZM) and optoelectronic oscillator are provided in [61-65], while a reconfigurable microwave photonic mixing architecture based on a dual-polarization MZM and a polarizer is achieved in [66].

It is interesting also to analyze some notably literature results in which the presented techniques are applied to satellite communications: the implementation of a breadboard demonstrator proof-of-concept containing a microwave-photonic frequency generation unit (FGU) and a frequency conversion unit (FCU), based respectively on a X-band dual-loop optoelectronic oscillator and on an electro-optical Mach-Zehnder modulator (EOM), optical amplifier (OA) and optical-to-electrical conversion (OE), is shown in [67]. In [68] the authors demonstate a satellite repeater with improved flexibility by the implementation of a frequency-conversion system capable to convert the input RF frequency to four different ones by adjusting modulators' electrical parameters (DP-MZMs) and needing only one frequency-fixed microwave source. In the same way authors in [69] propose a flexible frequency conversion method based on optical frequency comb (OFC) for satellite repeater applications, in which a dual-driven Mach-Zehnder Modulator (DMZM) is driven by the received RF signal to perform SSB modulation and two dual-parallel MZMs (DP- MZMs) are used to generate two coherent OFCs. Another scheme for a microwave photonic repeater system is achieved in [70] where simultaneous multi-band frequency conversion with only one frequency-fixed microwave source are obtained. The scheme employs one 20 GHz bandwidth dual-drive Mach-Zehnder modulator (MZM) and two 10 GHz bandwidth MZMs and prevents generating interference sidebands by using two optical filters after optical modulation. A multiple broadband simultaneous radio frequency (RF) down-conversion switching schema, in different bands and different intermediate frequency (IF) channels, for satellite communication is obtained in [71], while authors in [72] demonstrate a satellite on-board processing method implementing photon frequency conversion. Finally a tunable microwave-photonic frequency converter with integrated photonic filters for unwanted optical carriers and sidebands suppression is described in [73], while authors in [74] propose a coherent photonic-aided payload receiver capable to up-convert signals coming from the receiving feeds into optical signals, separate all the beams via beamforming and finally down-convert them back into radio frequency signals to be retransmitted towards ground.

3.2 Proposed architecture and principle of operation

Figure 3.2 shows the conceptual representation of the architecture of the proposed hybrid microwave/photonic WDM multiple local oscillators RF frequency down converter.

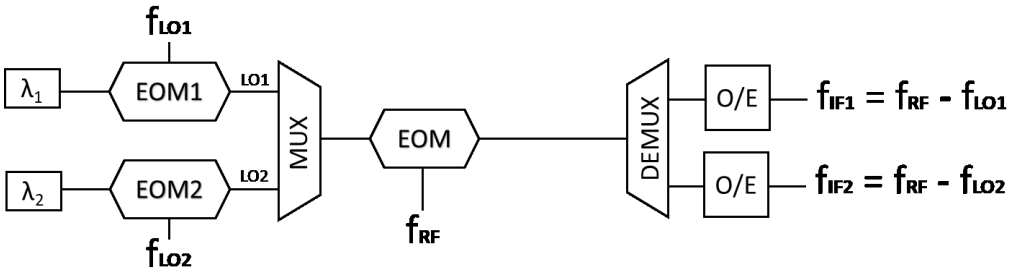

Figure 3.2: WDM multiple-LOs RF down converter

Single-tone signals at frequencies f_{LO1} and f_{LO2} are applied, respectively, to the electro-optical modulators EOM1 and EOM2 to modulate the continuous laser sources with optical fields E_{CW1} and E_{CW2}. The values of the optical fields at the output of EOM1 and EOM2 are given by [75]:

$$LO1 = E_{EOM1} = cos\left[\frac{\pi}{2}\frac{Vcos(2\pi f_{LO1}t + V_{bias})}{V_\pi}\right]E_{CW1}$$

$$LO2 = E_{EOM2} = cos\left[\frac{\pi}{2}\frac{Vcos(2\pi f_{LO2}t + V_{bias})}{V_\pi}\right]E_{CW2}$$

where V_π indicates the modulators switching voltage and V_{bias} indicates the modulator biasing voltage. Once multiplexed, the two optical local oscillator signals LO1 and LO2 feed the input of the EOM to which the RF single tone signal f_{RF} is applied to be down-converted. The optical field at the output of this stage is given by:

$$E_{TOT} = cos\left[\frac{\pi}{2}\frac{Vcos(2\pi f_{RF}t + V_{bias})}{V_\pi}\right](E_{EOM1} + E_{EOM2})$$

By applying Werner formulas, the above relation can be rewritten as:

$$E_{TOT} = \frac{1}{2}\sum_{i=1}^{i=2}\left\{\cos\left[\frac{\pi V}{2V_\pi}(\cos(2\pi f_{RF}t + V_{bias}) - \cos(2\pi f_{LOi}t + V_{bias}))\right] + \cos\left[\frac{\pi V}{2V_\pi}(\cos(2\pi f_{RF}t + V_{bias}) + \cos(2\pi f_{LOi}t + V_{bias}))\right]\right\}E_{CWi}$$

where the sum over the i-index is extended to all the photonic local oscillators composing the multiplexed signal (in this simple case LO1 and LO2). By expressing all the above cosines as complex exponentials and expanding them according to Jacobi-Anger identities, it can be shown that the optical spectra of the two photonic optical oscillators are mixed with the RF signal, as represented in Figure 3.3.

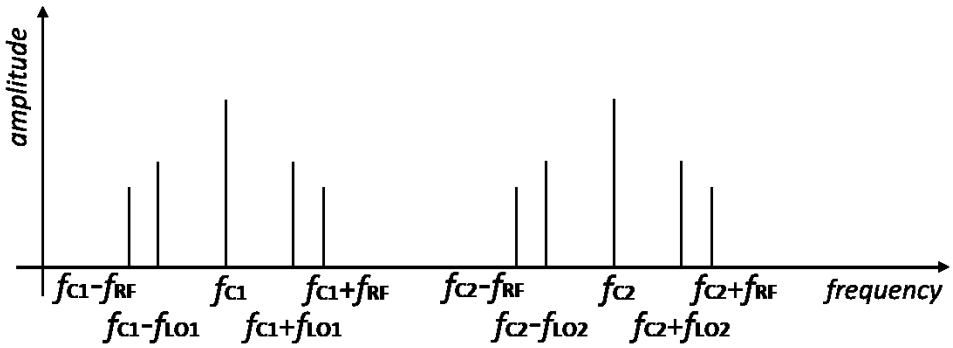

Figure 3.3: Optical spectra of two LOs mixed with the RF signal.

As shown, the obtained optical spectra contain the lines corresponding to the two optical carriers and the lines corresponding to the sum and difference frequencies between each optical carrier and the RF and LOs signals.

After wavelength separation, by means of the WDM DEMUX, each optical signal is sent to one photodetector where the AC term of the photocurrent is expressed by [55]:

$$i_{AC} \propto -J_1(\beta_1)J_0(\beta_2)\sin\phi_0\cos(\omega_{RF}t) + J_1^2(\beta_1)\cos(2\omega_{RF}t) + J_1(\beta_2)J_0(\beta_1)\sin\phi_0\cos(\omega_{LO}t) + J_1^2(\beta_2)\cos(2\omega_{LO}t) + J_1(\beta_1)J_1(\beta_2)\cos\phi_0\cos((\omega_{RF}-\omega_{LO})t) + J_1(\beta_1)J_1(\beta_2)\cos\phi_0\cos((\omega_{RF}+\omega_{LO})t) + \cdots$$

where J_n are the n^{th}-order Bessel functions of the first type, ϕ_0 is the phase difference between the two arms due to the bias, and β_1 and β_2 are the modulation indexes associated to the signals RF and LO, respectively.

As can be seen this current contains contributions related to the harmonics of the local oscillator and the RF signal and their sum and difference frequencies: an adequate electrical filtering allows to select the IF one.

3.3 System simulation and performance evaluation

The RF frequency down converter described in the prevous secion has been simulated exploiting the commercial OPTISYSTEM simulation tool.

The implemented schematic is based on two electronic local oscillator f_{LO1} and f_{LO2} at different frequencies, respectively 10.1 GHz and 14.1 GHz. They are used to externally modulate the optical signal from two continuous wave lasers at different wavelenght, λ_1 at 1553 nm (193.1 THz) and λ_2 at 1551 nm (193.3 THz) respectively, with an output optical power of 30 mW. These two resulting photonic local oscillators LO1 and LO2 are multiplexed by the WDM 2x1 MUX and finally used to feed a dual port MZM biased at quadrature point. This modulator is driven by the RF signal to be

down converted. Finally the two optical channels are separated by the WDM 1x2 DEMUX and each of them is detected by a pin photodiode and the resulting electrical signal is filtered.

In order to demonstrate the effective operation of the photonic WDM down-converter, we have down converted a BPSK signal. Indeed BPSK is representative of the constant envelope modulation schemas which are the most utilized in satellite communications since they minimize the effect of nonlinear amplification in High Power Amplifiers (HPAs).

Figure 3.4 shows the BPSK transmitting section to be connected to the RF input port of the EOM.

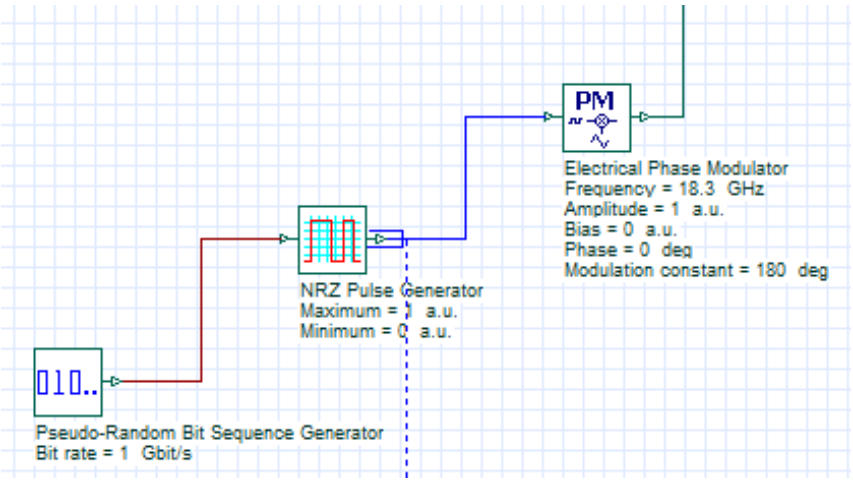

Figure 3.4: Transmitting section for the BPSK demonstration

It is composed by a pseudo-random bit sequence generator at 1 Gbps driving a NRZ pulse generator. In turn, the obtained modulating signal drives an electrical phase modulator providing a sinusoidal carrier at 18.3 GHz, whose phase changes of 180° are related to the input signal amplitude (i.e. NRZ pulses). The obtained BPSK modulated waveform represents the RF signal to be down-converted by the dual-port Mach-Zehnder modulator, fed by the two photonic local oscillators LO1 and LO2.

Instead the BPSK receiving section is connected to the output corresponding to the local oscillator LO2 at 1551 nm (193.3 THz) of the photonic frequency converter and it is shown in Figure 3.5.

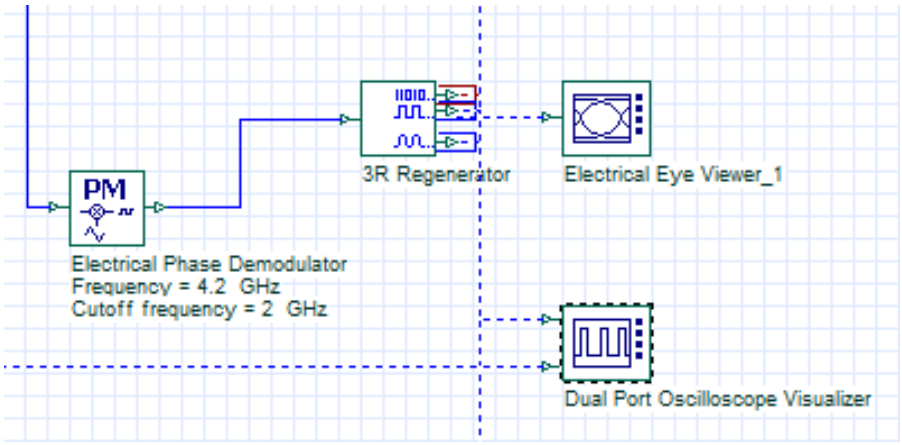

Figure 3.5: Receiving section for the BPSK demonstration

After photodetection and band-pass filtering, the frequency down-converted signal has a spectrum centred at the IF frequency of 4.2 GHz (considering the local oscillator LO2 which corresponds to the frequency f_{LO2} equals to 14.1 GHz), as shown in Figure 3.6. This received electrical signal is processed by the BPSK demodulator and the output base-band signal sent to a 3R regenerator for re-timing and re-shaping of the received pulses, as in Figure 3.5.

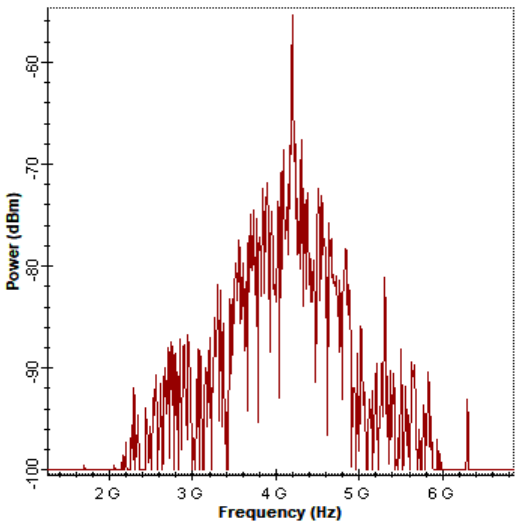

Figure 3.6: Electrical spectrum of the down converted binary BPSK signal.

Finally Figure 3.7 shows the transmitted (blue line) and received (red line) baseband NRZ signals, representing the transmitted and received sequences of bits.

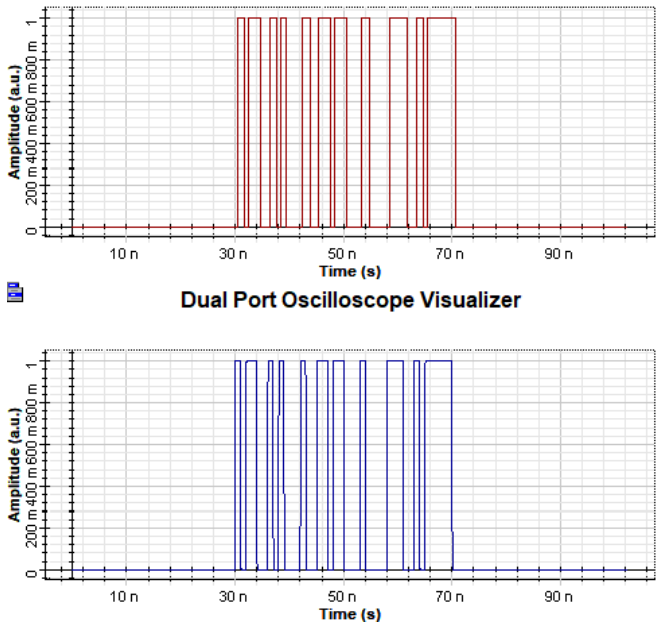

Figure 3.7: Received (red line) and transmitted (blue line) NRZ pulses.

As can be noticed, a good match between them has been obtained. The estimated min BER (defined as the minimum value for the bit error rate evaluated in the eye time window) value is 10^{-5} by considering that in the analyzed system forward error correction (FEC) techniques have not been applied. By exploting WDM the proposed down-conversion scheme improves frequency conversion scalability by addition of further wavelenghts. Another improvement in the performance of the proposed scheme can be achieved by adding an optical amplifier (AO) to compensate the mixer conversion losses.

4. Optical Butler Matrix for beamforming in hybrid microwave/photonic SATCOM payload

Antenna beamforming is the second operation implemented on a SATCOM payload to be considered, in this thesis work, for implementation in the optical domain. In particular this chapter [76] will investigate two configuration of symmetric 4x4 and 8x8 optical Butler matrices, both operating at 1.55 μm and based on hybrid couplers and phase shifters. These building blocks have been implemented, for simulation purpose, in Silicon on Insulator (SOI) technology; Beam Propagation Method (BPM) has been exploite for design demonstration and performances evaluation.

4.1 Technological state-of-the-art overview

Beamforming is a key technology utilized in satellite communication systems to enhance the efficiency of transmissions and receptions. This technology is designed to selectively focus radio frequency (RF) energy in a specific direction, thereby increasing signal power in that direction and reducing interference from other directions. Beamforming can be implemented in both the transmission and reception domains, and is particularly useful for optimizing coverage and transmission capacity in specific areas. Its main advantages are:

- **Increased spectral efficiency**: beamforming allows satellites to focus their signals on specific areas, reducing interference and improving spectral efficiency. This targeted approach enables the use of available frequency spectrum more effectively.
- **Enhanced coverage precision**: satellites employing beamforming can precisely shape and direct their coverage areas. This enables operators to tailor their services to specific regions, optimizing connectivity and resource allocation.
- **Improved signal quality**: by concentrating energy in desired directions and minimizing interference, beamforming enhances signal quality. This results in a more reliable and consistent communication experience for users on the ground.
- **Flexibility in network management**: dynamic beamforming enables satellites to adapt to changing network conditions, allowing for real-time adjustments to optimize performance. This flexibility is crucial for managing varying user demands and environmental factors.
- **Mitigation of interference**: beamforming technology helps mitigate the effects of interference from other satellites or terrestrial sources. This interference reduction contributes to a cleaner and more robust communication environment.

- **Optimized resource utilization**: satellites equipped with beamforming capabilities can focus their transmission resources where they are needed most. This results in efficient resource utilization, reducing wastage and maximizing the overall capacity of the satellite.
- **Point-to-point connectivity**: beamforming facilitates point-to-point connectivity, enabling satellites to establish strong and direct communication links with specific ground stations or user terminals. This is particularly valuable for applications requiring dedicated and reliable connections.
- **Adaptive to user movements**: some beamforming systems can dynamically track the movement of users or objects on Earth. This adaptability ensures that the satellite maintains a continuous and stable connection, even when users are on the move.
- **Cost-effective targeting**: by concentrating resources in specific areas, satellites can provide targeted services without the need for excessive power or bandwidth. This targeted approach can lead to cost savings in terms of satellite design, operation, and maintenance.
- **Support for Various Applications**: beamforming enables satellites to support a diverse range of applications, from broad-scale broadcast transmissions to specialized services requiring high data rates and low latency. This versatility makes satellites equipped with beamforming suitable for a wide array of communication needs.

On the other hand the main limitations are linked to:

- **Technical complexity**: implementing beamforming requires sophisticated hardware and software, increasing the overall complexity of the system.
- **High costs**: advanced antenna arrays and control electronics can incur high design, development, and implementation costs.

In this sense photonic beamforming (PBF), by exploiting photonic components to manipulate and control radiofrequency (RF) signals, represents a possible approach to overcome the main limitations of traditional electronic beamforming, especially in applications such as radar systems, wireless communication and obviously satellite communication. PBF allows to change indirectly a radio frequency on an optical carrier and to directly manipulate a light signal for satellite communications, radar, 5G communications, visible light communications, optical communications, lidar and so on [77-80]. Moreover, respect to their electrical/RF counterparts, PBF allows to achieve much higher available bandwidth and significantly reduced weight, size and power consumption. The authors in [81] describe the benefits of microwave photonic beamforming applied to broadband Active Phased Antenna Array (APAA): low and frequency-undependant propagation losses, stability and

predictability of the signal phase, electrical isolation. In [82] it has been demonstrated an integrated optical beamforming network capable to control the reception angle of 36 independent beams in Ku-band by employing a phased array receive antenna with 144 antenna elements and a comparison with an equivalent RF-BFN in terms of size, footprint, mass, vibration sensitivity, tunability, RF-crosstalk and cost is done.

Generaly speacking, the main beamforming technology is based on antenna array systems, constituted essentuially by the radiating antenna elements and the beamforming network (BFN). Is such a system each antenna element is fed by a signal with specific magnitude and phase, so that the required radiation pattern is determined by the progressive phase delay across the array elements.

There are mainly three approaches to beamforming [83], as summarized and explained in Figure 4.1.

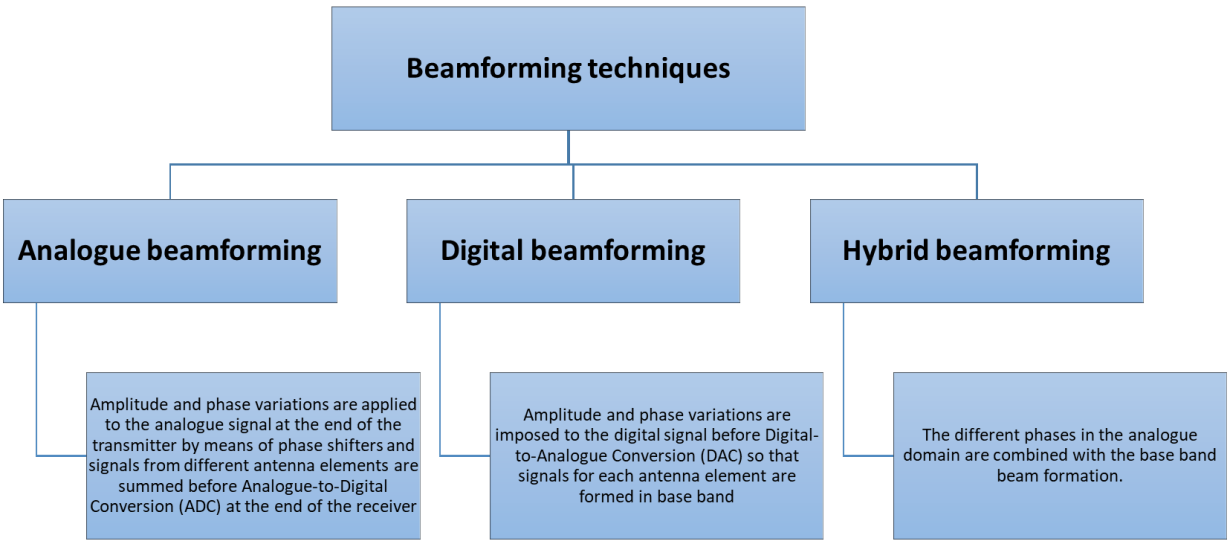

Figure 4.1: Beamfoming techniques overview [83]

In digital beamforming the main limitation is due to the high mass and power requirements of the digital beamformer processor which increase proportionally to the increase of the number of feed elements and bandwidth per feed [82]; In addition in case of wide-band systems with a huge number of antenna elements, digital beamforming leads to high power consumption due to the large number of DACs and ADCs, not required in the analogue solution [84]. For this resons often analogue beamforming can be a suitable solution, especially for space applicatons (due to the mass and power requirements): in this case the feeding network of such as analogue beamforming architecture is required to low cost, lossless, simple circuit-bas edand with a minimum number of components.

In general, feeding network architectures are divided into three main categories, according to the feeding method: the series-feed, parallel-feed, and matrix feeding [85-86]. The most widely known

beamforming matrices are the Butler [87], Blass [88] and Nolen [89] matrices. The matrices above can be compared by taking in account some figures of merit such as required hardware components, operative degree of freedom, efficiency, power loss and ease of design [90]. Instead in [91] a review of their main design features and the comparison of the achieved performance results are provided, in addition to the identification of the main advantages and drawbacks related to several particular configurations retrieved in literature. A summary of the main features characterizing Butler, Blass and Nolen matrices are provided in Table 4.1.

Table 4.1: Comparion between Butler, Blass and Nolen matrices.

BUTLER MATRIX	BLASS MATRIX	NOLEN MATRIX
• The Butler matrix exploits a parallel multiple beam feed method. • The Butler matrix is designed with a symmetrical structure, i.e. an equal number of input (beam) and output (antenna) ports (N × N). • Lower flexibility since it is constrained to have an equal number of ports for input and output, being this number a power of 2. • The Butler matrix is composed by hybrid couplers, crossovers and phase shifters. • The Butler matrix is preferred due to its low architectural complexity and its ease of design. • Best performance in terms of power loss and efficiency. • Reduced number of utilized components.	• The Blass matrix exploits the series feed method. • The Blass matrix can be designed with an unequal number of inputs and outputs (M × N). • More flexibility since there are no constraints to have an equal number of input/output ports. • The Blas matrix is composed by couplers, phase shifters and load terminations, while it does not require any crossover. • Increased architectural complexity and lower ease of design. • Higher power loss and lower efficiency with respect to Butler matrix. • Higher number of utilized components with respect to Butler matrix.	• The Nolen matrix exploits the series feed method. • The Nolen matrix can be designed with an unequal number of inputs and outputs (M × N). • More flexibility since there are no constraints to have an equal number of input/output ports. • The Nolen matrix is designed by cutting the Blass matrix along the diagonal line and it requires only couplers and phase shifters. • Increased architectural complexity and lower ease of design. • Higher power loss and lower efficiency with respect to Butler matrix. • Higher number of utilized components with respect to Butler matrix.

Focusing on the Butler matrix, it has widely considered in literature and exploted in a variety of applications. Considering its simmetrical architecture, it has been proposed in different configurations, i.e. 4×4, 8×8 and 16×16 [92-94]. In addition, also some unsymmetrical configurations have been proposed, such as 2×4 [95], 3×4 [96-97] and 4×8 [98-99]. Other demonstrated features are dual-band [100], compact size [101], broadband [102], low loss [103], sidelobe control [104], flexibility [105] and beam steering [106-107]. Some papers have also reported Butler matrices

configurations with both an equal and an unequal number of inputs and outputs and implementing Low Sidelobe Level (SLL) distributions [108-109].

All the above cited works mainly consider the implementation of the Butler matrix in the electrical domain. Only few works focusing on optical Butler matrix networks have been issued in the past, mainly demonstrating the achieved improvements in terms of smaller size and wider bandwidth compared with the electrical ones [110-112].

Finally a simple photonic-assisted Butler matrix network using low-cost intensity-modulation direct-detection (IMDD) has been demonstrated in [113], in which the passive phase control is for RF signal transmitted on the optical carrier, instead of the phase of the optical carrier itself.

4.2 Butler matrix proposed architectures and operations

The architecture of a Butler matrix in composed by the following building-blocks:

- **3 dB couplers with shift of 90°:** they ensure that antenna system elements are fed with equal values of power.
- **Crossovers:** they impement transmission lines overlaps by ensuring signal purity.
- **Phase shifters:** they provide the necessary phase shift needed for beam formation in the desired direction.

The 3dB couplers are positioned in cascade and connected to each other by fixed-value phase shifters implemented by means of transmission lines with different lengths.

When a square architecture Butler matrix is considered (i.e. symmetrical structure), the number of input ports is equal to the number of output ports: this number of ports is given by $N = 2^n$ where n is the number of devices placed in cascade in the square matrix. It follows that the Butler matrix is composed by $\frac{N}{2} log_2 N$ couplers and $\frac{N}{2} log_2 (N-1)$ phase shifters (less than the number of couplers and phase shifters required by the other beamforming matrices).

The simplest multibeam device is based on a single hybrid coupler. As the order of the Butler matrix increases, its architecture becomes more complex due to the fact that successive levels of directional couplers and phase shifters need to be included between the two primary levels, i.e. the more external ones.

4x4 Butler matrix

The first architecute considered in this work is the 4x4 Butler matrix, composed by one crossover, four hybrid couplers and two 45° phase shifters. In Figure 4.2 the schematic of the 4x4 Butler matrix is reported: it is constituted by a cascade of hybrid couplers 2x2 connected to each other by delay lines equal to $\lambda/(2N) = \lambda/8$, being N the number of ports, which corresponds to a phase shift of $\pi/4 = 45°$.

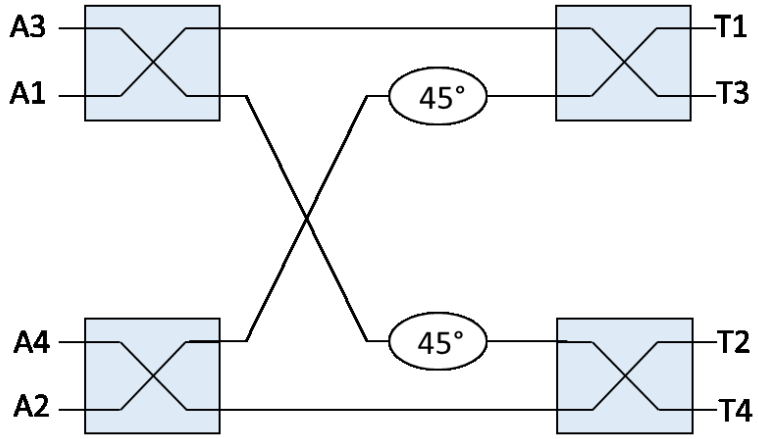

Figure 4.2: Block diagram of a 4 x 4 Butler matrix

The 4x4 Butler matrix operates according to the selection rules provided in Table 4.2, showing the initial phase shifts to be provided to the inputs A1, A2, A3, A4 to select the desired output among T1, T2, T3, T4 (for example if A1=135°, A2=0°, A3=225°, A4=90°, the selected output port is T1).

Table 4.2: Phase shift relationships for a 4 x 4 Butler matrix

	A1	**A2**	**A3**	**A4**
T1	135	0	225	90
T2	180	135	90	45
T3	45	90	135	180
T4	90	225	0	135

8x8 Butler matrix

The second architecure considered in this work is the 8x8 Butler matrix, composed by 10 crossovers, 12 hybrid couplers and 8 overall phase shifters, 2 of which provide a phase shift of 67.5°, other 2 provide a phase shift of 22.5° and the last 4 provide a phase shift 45°. In Figure 4.3 the schematic of the 8x8 Butler matrix is also reported.

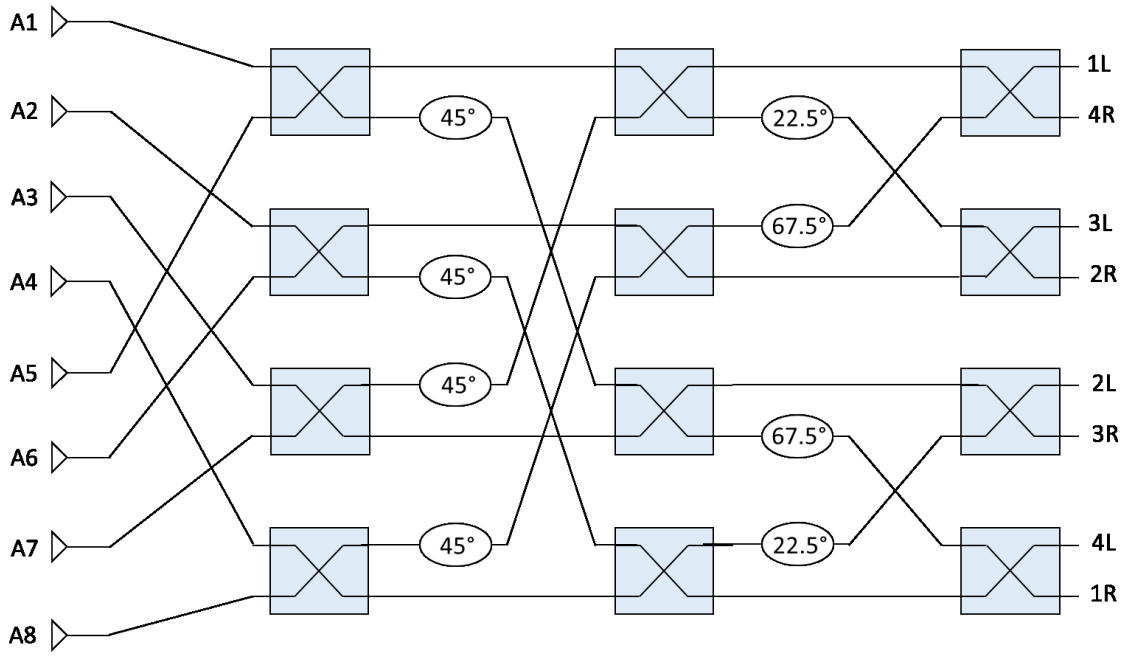

Figure 4.3: Block diagram of a 8 x 8 Butler matrix

As in the previous case, Table 4.3 shows the phase relationship distribution of the 8x8 Butler matrix.

Table 4.3: Phase shift relationships for a 8 x 8 Butler matrix

	Beam Ports							
Ant. Ports	**1L**	**4R**	**3L**	**2R**	**2L**	**3R**	**4L**	**1R**
A1	90	-180	157.5	-112.5	135	-135	157.5	-112.5
A2	112.5	22.5	-90	-180	-157.5	112.5	-45	-135
A3	135	-135	22.5	112.5	-90	0	112.5	-157.5
A4	157.5	67.5	135	45	-22.5	-112.5	-90	-180
A5	-180	-90	-112.5	-22.5	45	135	67.5	157.5
A6	-157.5	112.5	0	-90	112.5	22.5	-135	135
A7	-135	-45	112.5	-157.5	-180	-90	22.5	112.5
A8	-112.5	157.5	-135	135	-112.5	157.5	-180	90

4.3 Design simulation and performance evaluation

For each of the previous introduced Butler matrices architectures the the desing features and the performance simulation results are provided. The analysis has been performed by means of the BeamPROP-RSoft, based on the Beam Propagation Method (BPM).

4x4 Butler matrix

The integrated optical 4x4 Butler Matrix has been designed by considering the Silicon on Insulator (SOI) technology at the operation wavelength of 1.55 μm. The silicon ridge waveguide is characterized by a refractive index equal to $n_{Si} = 3.48$, width of 0.5 μm and height of 0.22 μm. The SiO_2 substrate has a refractive index $n_{SiO2} = 1.45$. The single mode $TE_{0,0}$ of the waveguide at the operating wavelength has a refractive effective index equal to $n_{eff} = 2.318$.

The implementation of the 4x4 integrated optical Butler matrix in the computation domain is represented in Figure 4.4. It is composed by four 2x2 hybrid couplers connected with delay lines corresponding to a phase shift of 45°, with length respectively $L_1 = 72$ μm and $L_2 = 79.6$ μm.

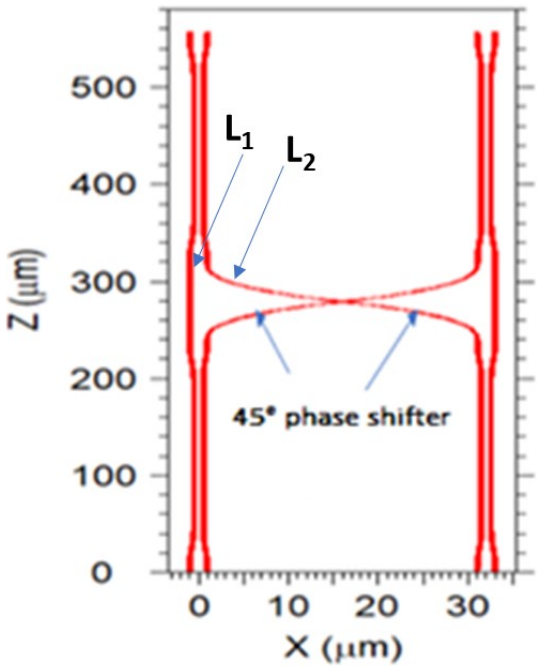

Figure 4.4: implementation of the 4x4 integrated optical Butler matrix

The required phase shift of $\Delta\varphi = k_0 \Delta_{neff} \Delta L$ can be obtained:

i) by varying the length of the two optical paths of the delay lines L_1 and L_2 but considering both the ridge waveguides with the same geometrical parameters (and therefore the same refractive effective index n_{eff}) or

ii) by varying the geometry (for example the ridge width) of one of the two waveguides, i.e. varying the refractive effective index n'_{eff}.

In the former case, considering the operation wavelength of 1.55 μm, the single mode refractive effective index n_{eff}=2.318 and the required $\Delta\varphi = \pi/4$, a value of the optical path difference $\Delta L = L_2 - L_1 = 0.0838$ μm has to be obtained.

In the latter case, assuming $L_1 = 72$ μm and $L_2 = 79.6$ μm, the required phase shift $\Delta\varphi = \pi/4$ can be obtained by assuming the width of the second waveguide equal to 0.4336 μm, for which the new refractive effective index n'_{eff} has been obtained by means of the equation $\Delta\varphi = k_0 (n'_{eff} L_2 - n_{eff} L_1)$ and it results equal to 2.097.

Table 4.4 reports the output power at each of the output ports, in the four configurations, as a percentage of the total input power, where 100% indicates the in-phase sum of four signals. The outputs showed in the table has been obtained by feeding the input ports with signals with appropriate initial phases as defined in Table 4.2. The non-ideality of the obtained results is mainly due to the crosstalk at the crossing point between the two L_2 waveguides.

Table 4.4: Power at output ports for each beam configuration as a percentage of the total input power

	Out1	**Out2**	**Out3**	**Out4**
T1	95.21	0.24	$6x10^{-2}$	$2.9x10^{-4}$
T2	0.46	94.9	0.13	$5.4x10^{-2}$
T3	$5.3x10^{-2}$	0.13	94.91	0.46
T4	$3x10^{-4}$	$5.9x10^{-2}$	0.24	95.22

For each T1, T2, T3, T4 configuration, most of the signal (around 95% of the overall input signal) propagates through the related output port Out1, Out2, Out3, Out4. The other outputs, which ideally should have zero power, exhibit a minimum of power, which means having a phase error on the other wave fronts. The device has a surface area of 34x558 μm^2.

8x8 Butler matrix

As in the previous case, a similar study has been performed on the integrated optical 8x8 Butler matrix, whose implementation is shown in Figure 4.5.

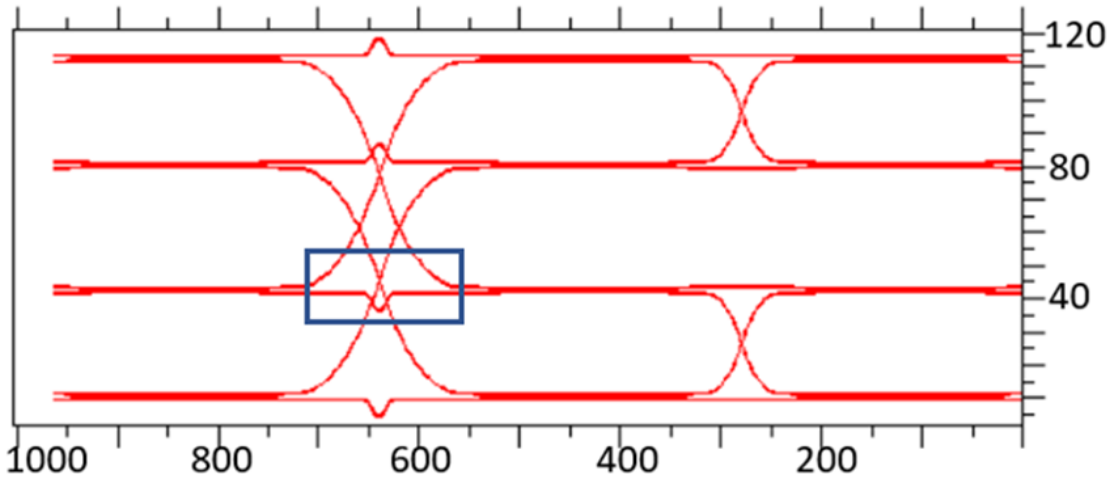

Figure 4.5: Implementation of the 8x8 integrated optical Butler matrix

Similarly to the considerations done for the previous case, a ridge waveguide caracterized by a width of 0.4315 μm, associated to a phase shift of 22.5°, has been considered; in the same way a width of 0.4348 μm has been considered for a phase shift of 67.5°. This is obtained considering that from the equation $\Delta\varphi = k_0 (n'_{eff}L_2 - n_{eff} L_1)$ the values of $n'_{eff} = 2.087$ for 22.5° while $n'_{eff} = 2.102$ for 67.5° are estimated. If the other approach is followed, according to the equation $\Delta L = \Delta\varphi/(k_0 n_{eff})$, for 22.5° the ΔL must be equal to 0.0419 μm, while for 67.5° a ΔL of 0.1257 μm is required.

A point of attention is represented by the various crossings of the waveguides: in fact when the second cascade of couplers is inserted, they must be designed in order to maximize the transmitted power and minimizie the crosstalk. It has been observed that the best crossing angle between two waveguides in S-Bend mode is equal to 45°. In fact a lower angle creates crosstalk, even for 22.5° the signal is completely coupled in the other waveguide. Instead, by increasing the angle of inclination of a single waveguide, the signal is lost as it tends to propagate in a straight line, with a limit case for 70°, where the signal couples out from the guide.

Finally the integrated optical 8x8 Butler matrix has been simulated by considering 8 signals of equal amplitude (normalized to 1) and phase shift relationships according to Table 4.3: for example, if the output A1 has to be activated, the appropriate phase shifts in the first row must to be applied to the related inputs of the matrix in Figure 4.3. The obtained results are reported in Table 4.4, containing

the achieved values of power of the 8 outputs, expressed as a percentage of the total input power, when the phase shift values of the input signals follow the configurations indicated in Table 4.3.

Table 4.5: Power of the eight outputs expressed as a percentage of the total input power

	A1	**A2**	**A3**	**A4**	**A5**	**A6**	**A7**	**A8**
1L	80.55	0.74	0.06	0.36	0.29	0.45	0.02	0.38
4R	0.54	74.52	0.64	0.09	0.33	0.92	1.38	0.09
3L	0.04	0.68	76.2	0.23	0.12	0.6	1.3	0.41
2R	0.45	0.01	0.25	80.86	0.43	0.04	0.42	0.67
2L	1.6	0.65	0.99	1.37	73.37	1.12	1.11	1.92
3R	0.41	1.29	0.59	0.12	0.24	76.17	0.69	0.04
4L	0.09	1.36	0.92	0.33	0.09	0.63	74.65	0.54
1R	0.38	0.02	0.44	0.3	0.35	0.05	0.74	80.48

The output power values range between 70% and 80% of the overall input power, while an ideal behaviour should show a percentage of signal equal to 100% at a single output for each configuration. This is due to th fact that in reality the various crossing points make the other matrix outputs not null. This translates into noise for the signal of that wavefront. The results obtained are very promising considering also that the device occupies a square area of 123x965 μm^2.

5. Optical circuit switching in WDM-based FSO SATCOM systems

Unlike the two previous sections, the present one is focused on the second typology of payload architecture introduced in the Chapter 2, i.e. the fully transparent optical payload. In particular this chapter [114] provideds a system functionality demonstration and performance evaluation of a Space OTN node exploiting an optical switching matrix to perform wavelength circuit switching of WDM channels.

As already introduced, a first implementation of a satellite system based on FSO communication can be found in the EDRS (European Data Relay System) constellation [17], while more recent studies, which are being conducted by ESA [49], are following the ambition to implement a Space-based OTN infrastructure capable to extend seamlessly into space the already existing high-capacity terrestrial optical network and to complement it, providing also optical connectivity to space assets located at different orbits. The future implementation of such system will bring new service and market opportunities:

- convergence of space infrastructures towards terrestrial networks, improving the overall network capacity and enlarging the capability towards new service and application (i.e. cloud in the sky, routing on-board satellite, 5G, etc);
- reduction of the Worldwide Digital Divide, offering large coverage with a low infrastructure implementation cost;
- reduction of the RF spectrum congestion;
- for the European sovereignty, reduction of the dependence from the fiber backbones providers that could potentially limit the transcontinental communication with their access limitations and costs.

The main components of a Space OTN architecure, as shown in Figure 5.1, are:

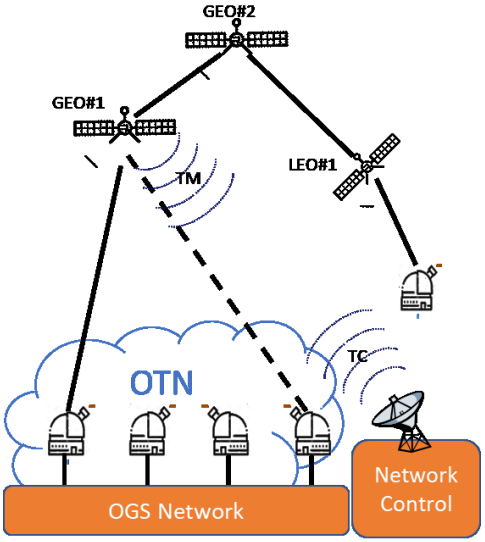

Figure 5.1: Space OTN architecture

- the **space nodes**, constituting the Space Segment (SS), with the capabilities to set high capacity optical links towards other nodes (both in space and on ground) and to perform on board signals switching/routing;
- the **ground nodes**, constituting part of the Ground Segment (GS), composed by Optical Ground Stations (OGSs) interconnected with the space nodes (via OFLs) and interconnected between themselves (OGSs networks) to improve the link availability by means of site diversity;
- the additional **ground elements** operating (management and control) both the space and the ground nodes and interfacing the Space OTN with the Terrestrial one.

The necessity of the use of Wavelength Division Multiplexing (WDM) technologies, as already done in terrestrial fiber networks, is justified by the fact that such system will rely on high capacity FSO links (from hundreds of Gbps to Tbps of user data rate) and multi-hop connectivity (i.e. to route a signal across different space/ground nodes). This translates into the necessity to manage switching/routing capabilities of optical signals on-board the satellite: in this sense the switching matrix represents one of the key building blocks of the system. For the sake of clarity, in Figure 5.2 the functional architecture of the considered reference payload is reported.

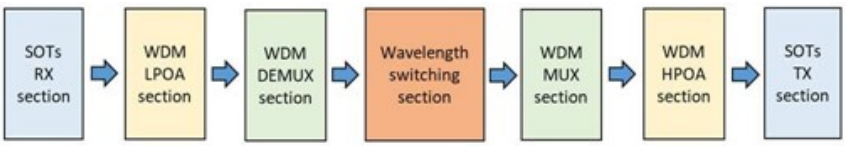

Figure 5.2: Functional architecture of the all optical payload

The main payload elements are:

- Satellite Optical Terminals (SOTs) supporting bidirectional (TX/RX) WDM channels;
- Optical amplifier sections, in particular the Low Power Optical Amplifier (LPOA) section performing the input low-noise pre-amplification of the RX signal and the High Power Optical Amplifier (HPOA) section performing the output booster amplification of the TX signal;
- Demultiplexing (DEMUX) and Multiplexing (MUX) sections of RX and TX WDM optical channels, respectively;
- Reconfigurable optical switching matrix (e.g. OXC or ROADM).

5.1 Technological state-of-the-art overview

There are many reasons for introducing optical switching in satellite payloads: the main important drivers are scalability to large port counts, lower mass and volume (compared to RF switches), transparency, RF isolation and suppression of EMI/EMC [115]. Several solutions and technologies for all-optical switching have been studied and proposed already for terrestrial communication networks, such as Opto-Mechanical Switches, Micro-Electro- Mechanical-Systems (MEMS) Switches, Electro-Optic Switches, Thermo-Optic Switches, Liquid-Crystal Switches, Bubble Switches, Acousto-Optic Switches, Magneto-Optic Switches, Semiconductor Optical Amplifiers (SOAs) Switches [116-119]. They show different performances with in terms of some important features such as switching time, insertion loss, crosstalk, extinction ratio, polarization dependent loss, reliability, power consumption, scalability, temperature resistance. But while in case of terrestrial applications most of all the above mentioned technologies translate into commercial off-the-shelf devices, this is no longer true when space applications are considered, since in this case they must to be designed developed, tested and finally qualified to perform in harsh environment. Only few activities have been developed in this sense: an ESA study [120] in which, starting from the definition of a set of space applications and scenarios, three swithching matrix technologies, i.e. Magneto-Optic, Bulk Electro-Optic and Waveguide Electro- Optic, have been selected for manufacture development and test campaign: in particular their performance in terms of insertion loss, crosstalk and switching speed have been evaluated and compared under test campaing (thermal vacuum cycles, vibration and shocks, gamma radiation test); instead another activity performed by EC [121] demonstrated the ruggedization to space environment of a proprietary HUBER+SUHNER Polatis technology, by means of the development and test of a breadboard.

5.2 Simulation scenario definition and simulation results

In order to perform the analysis, a simulation scenario has been established: it is based on a GEO reference satellite (hosting the switching matrix) capable to establish four kinds of different free space optical links:

- one OISL from a LEO to the GEO satellite (LEO altitude: about 1200 km and link distance: about 45000 km);
- two OFLs from two generic OGSs on ground (e.g. modelling the primary link and the handover one) to the GEO satellite (GEO altitude: 35786 km and link distance: 35786 km since both link performances have been evaluated for simplicity at 90° of elevation angle in first approximation);
- one additional OFL (modelling e.g. the connectivity towards an isolated OGSs (i.e. not in site-diversity) with the same parameters as above.

The communication features of this reference scenario are summarized in the following tables, according to the link budget analysis activity in [122]. In particular Table 1 provides the link budget for the OISL between GEO and LEO while Table 2 provides the link budget for the GEO OFL. Each free space link has been considered composed by 10 DWDM channels in C band (around 1550 nm) and with a channel spacing of 50 GHz, according to the ITU-T G.694.1 standard [123].

Table 5.1: Link budget for LEO-GEO OISL [121]

Link distance [km]	**45000**	**45000**
TX diameter [mm]	**400**	**130**
TX fixed Losses [dB]	-1	-1
Propagation Losses [dB]	-67.3	-67.3
RX fixed Losses [dB]	-1	-1
Minimum Required TX Power/λ [dBm]	**33.5**	**29**

Table 5.2: Link budget for GEO OFL [121]

Link distance [km]	**35786**	
	Uplink	**Downlink**
RX diameter [mm]	**400**	**600**
TX fixed Losses [dB]	-3	-1
Propagation Losses [dB]	-52	-52
Fiber coupling Losses [dB]	-1.9	-0.2
Total Link Losses [dB]	67.4	-64.3
TOT. MIN. REQUIRED TX POWER [dBm]	**33.4**	**30.3**

The simulation has been performed by means of the OptiSystem tool. With reference to the link budget summary above, the values of Minimum Required TX Power and Total Link Losses identified are exploited to set the power of the optical transmitters and the attenuation of the optical attenuators, respectively, in the simulation schematic: in fact each attenuator models the effects of all the losses

for each considered link. This allows to determine the received power at the input of each link (before the pre-amplification stage): considering that $P_{RX}[dBm] = P_{TX}[dBm] - L_{TOT}[dB]$, for all the links the total received power at each input port (of the GEO reference payload) is between -35 dBm and -34 dBm.

Then, the overall signal level associated to each link is ampified by means of a Low-Noise Pre-Amplifier: the parameters considered in the OptiSystem model for this block are the optical gain set to 26 dB and the Noise Feature set to 4. Subsequently, each signal is demultiplexed in order to separate all the WDM channels beloning to each link (10 channels per link): in particular a NRZ OOK modulated channel with a bit rate of 10 Gbps (100 Gbps of aggregated bitrate) has been considered for the simulation scenario purposes. In more detail this modulated signal is obtained by means of a Mach-Zehnder modulator fed by a CW laser source. In the simulation schematic the DEMUX component has been modelled as an ideal block (the same has been considered also for the MUX). At this point all the extracted WDM channels (40 channels) are given in input to a 40×40 Optical Switch Matrix Block performing optical channel circuit switching. The main parameters considered in the simulation schematic for this block are the insertion loss, set to 1.5 dB and the switching time set to 25 ms. After being routed, the channels at the output ports of the Switching Matrix are multiplexed again and boosted (High Power Optical Amplifier block) before being re-transmitted (similar observation already done for the RX section of the payload can be done for the TX one).

To evaluate the effects of the propagation of the signal through the free-space link and within the optical payload, a single WDM channel is extracted and photodetected on-board in order to evaluate the achieved communication performances: this simplified scenario is representative of one in which a customer payload is hosted on the same platform of the optical one. In Figure 5.3 the Eye Diagram from the photodetected signal associated to the 194.1 THz WDM channel (associated to one of the OFLs) is shown.

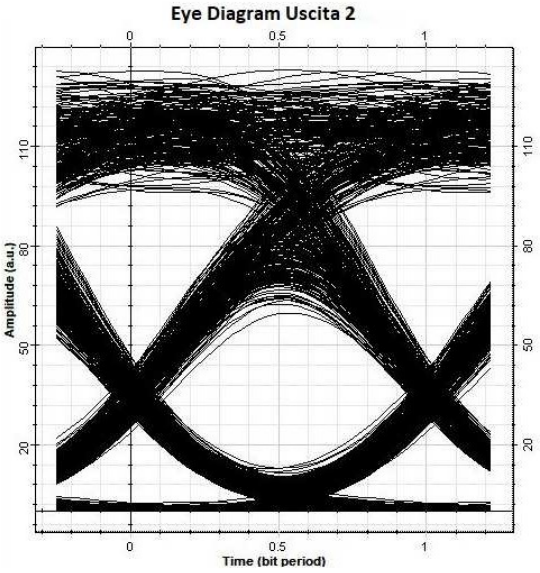

Figure 5.3: Eye Diagram of the NRZ signl associated to 194.1 THz optical channel.

From the Eye Diagram analyzer a minimum BER of the order of 10^{-7} is obtained, which is a meaningful result taking in account that no on board regeneration and processing of the signal (e.g. Forward Error Correction encoding, interleaving, turbulence mitigation, etc.) has been implemented to overcome propagation impairments.

6.Conclusions

The analysis of the current scenarios and future trends of SATCOM shows a new way to conceive space connectivity, in relationship with new potential services and market opportunities: satellite communications are becoming something closer to consumer needs, making SATCOM systems interconnected and interoperable with other different telecommunication infrastructures, such as terrestrial fixed and mobile networks (integration) and providing services to different typologies of final users, both in space and on ground (heterogenity). This leads to a sort of "three-dimensional" vision of concept to access space networks, more extensive with respect to how it has been experienced up to now. To allow this various enabling technologies are being developed, covering several levels of implementation, such as physical level, protocol level, service and security levels. In this context optical/photonic technologies play an important role, with the aim to overcome the current limitation of classical electronic technologies in terms of complexity and needed on-board resources and to build a space telecommunication infrastructure similar to the already existing terrestrial fiber-based one. This thesis work fits into this line of research and, starting from the identification of some SATCOM payload architectures, has provided an applicability study and a system demonstration of a set of on-board functionalities implemented in the optical domain. This represents a preparatory work for future developments which can include several different activities: the qualification for the space environment of already existing photonic devices with a proven heritage in terrestrial application; the design of new components and complex subsystems suitable for space applications by integrating a set of devices, performing different basic functionalities, on the same platform (Photonic Integrated Circuits, PICs); the improvement of architectures and protocols to overcome issues related to FSO space systems; finally the set-up of dedicated In-Orbit Demonstration (IoD) missions to demonstrate in space obtained technologies and operational concepts.

List of figures

List of tables

Bibliography

[1] G. Maral, M. Bousquet, SATELLITE COMMUNICATIONS SYSTEMS - Systems, Techniques and Technology; Fifth Edition, John Wiley & Sons Ltd, 2009.

[2] Charles C. Wang, Tien M. Nguyen, Gary W. Goo, Satellite payload architectures for wideband communications systems, Proceedings of MILCOM 1999, October 1999.

[3] R. Swinford, B. Grau, High Throughput Satellites - Delivering future capacity needs, Arthur D. Little, 2015, http://www.adlittle.de/uploads/tx_extthoughtleadership/ADL_High_Throughput_Satellites-Main_Report_01.pdf

[4] Michael Schneider, Christian Hartwanger, Helmut Wolf, Antennas for multiple spot beam satellites, CEAS Space Journal, December 2011, Volume 2, Issue 1 - 4, pp 59–66, Springer.

[5] Y. Henri, "The OneWeb satellite system." Handbook of Small Satellites: Technology, Design, Manufacture, Applications, Economics and Regulation. Cham: Springer International Publishing, 2020. 1091-1100.

[6] https://www.starlink.com/technology

[7] https://www.telesat.com/leo-satellites

[8] https://www.aboutamazon.com/what-we-do/devices-services/project-kuiper

[9] N. Pachler, I. del Portillo, E. F. Crawley and B. G. Cameron, "An Updated Comparison of Four Low Earth Orbit Satellite Constellation Systems to Provide Global Broadband," 2021 IEEE International Conference on Communications Workshops (ICC Workshops), Montreal, QC, Canada, 2021, pp. 1-7, doi: 10.1109/ICCWorkshops50388.2021.9473799.

[10] H. Xie, Y. Zhan, G. Zeng and X. Pan, "LEO Mega-Constellations for 6G Global Coverage: Challenges and Opportunities," in IEEE Access, vol. 9, pp. 164223-164244, 2021, doi: 10.1109/ACCESS.2021.3133301.

[11] B. Al Homssi et al., "Next Generation Mega Satellite Networks for Access Equality: Opportunities, Challenges, and Perfor-mance," in IEEE Communications Magazine, vol. 60, no. 4, pp. 18-24, April 2022, doi: 10.1109/MCOM.001.2100802.]

[12] N. Karafolas, "Optical Satellite Networking: The Concept of a Global Satellite Optical Transport Network." Near-Earth Laser Communications, Second Edition (2020): 401-428.

[13] V. W. S. Chan, "Optical Satellite Networks," J. Lightwave Technol. 21, 2811- (2003)

[14] N. Karafolas and S. Baroni, "Optical Satellite Networks," J. Lightwave Technol. 18, 1792- (2000)

[15] A. U. Chaudhry and H. Yanikomeroglu, "Free Space Optics for Next-Generation Satellite Networks," in IEEE Consumer Electronics Magazine, vol. 10, no. 6, pp. 21-31, 1 Nov. 2021, doi: 10.1109/MCE.2020.3029772.

[16] A. Carrasco-Casado, R. Mata-Calvo, (2020). Space Optical Links for Communi-cation Networks. In: Mukherjee, B., Tomkos, I., Tornatore, M., Winzer, P., Zhao, Y. (eds) Springer Handbook of Optical Networks. Springer Handbooks. Springer, Cham. https://doi.org/10.1007/978-3-030-16250-4_34

[17] ESA EDRS Program, online available: http://telecom.esa.int/telecom/www/object/index.cfm?fobjectid=29643

[18] H. Hauschildt, F. Garat, H. Greus, K. Kably, J.P. Lejault, H. L. Moeller, et al., "European Data Relay System - one year to go", Proceedings of ICSOS 2014 (International Conference on Space Optical Systems and Applications), May 7–9, 2014.

[19] H. Hauschildt, S. Mezzasoma, H. L. Moeller, M. Witting and J. Herrmann, "European data relay system goes global", 2017 IEEE International Conference on Space Optical Systems and Applications (ICSOS), pp. 15-18, 2017.

[20] A. U. Chaudhry and H. Yanikomeroglu, "Laser Intersatellite Links in a Starlink Constellation: A Classification and Analysis," in IEEE Vehicular Technology Magazine, vol. 16, no. 2, pp. 48-56, June 2021, doi: 10.1109/MVT.2021.3063706.

[21] G. Jansson, "Telesat Lightspeed™- Enabling Mesh Network Solutions for Managed Data Service Flexibility Across the Globe," 2022 IEEE International Conference on Space Optical Systems and Applications (ICSOS), Kyoto City, Japan, 2022, pp. 232-235, doi: 10.1109/ICSOS53063.2022.9749709.]

[22] M. Toyoshima, "Recent Trends in Space Laser Communications for Small Satellites and Constellations," in Journal of Lightwave Technology, vol. 39, no. 3, pp. 693-699, 1 Feb.1, 2021, doi: 10.1109/JLT.2020.3009505.

[23] S. Durante, L. Rodio, V. Schena, G. Calò, A. D'Orazio and V. Ferrara, "A system demonstration of optical circuit switching in a space-based WDM Optical Transport Network," 2023 IEEE 10th International Workshop on Metrology for AeroSpace (MetroAeroSpace), Milan, Italy, 2023, pp. 633-637, doi: 10.1109/MetroAeroSpace57412.2023.10190029.

[24] N. Saeed, A. Elzanaty, H. Almorad, H. Dahrouj, T. Y. Al-Naffouri and M. -S. Alouini, "CubeSat Communications: Recent Advances and Future Challenges," in IEEE Communications Surveys & Tutorials, vol. 22, no. 3, pp. 1839-1862, thirdquarter 2020, doi: 10.1109/COMST.2020.2990499.

[25] L. Sining, P. I. Theoharis, R. Raad, F. Tubbal, A. Theoharis, S. Iranmanesh, S. Abulgasem, M. U. Ali Khan and L. Matekovits. 2022. "A Survey on CubeSat Missions and Their Antenna Designs" Electronics 11, no. 13: 2021. https://doi.org/10.3390/electronics11132021

[26] C. Cappelletti, D. Robson, CubeSat missions and applications, in: Chantal Cappelletti, Simone Battistini, Benjamin K. Mal-phrus, Cubesat Handbook, Academic Press, 2021, Pages 53-65, ISBN 9780128178843, https://doi.org/10.1016/B978-0-12-817884-3.00002-3.

[27] M. Giordani and M. Zorzi, "Non-Terrestrial Networks in the 6G Era: Challenges and Opportunities," in IEEE Network, vol. 35, no. 2, pp. 244-251, March/April 2021, doi: 10.1109/MNET.011.2000493

[28] S. Liu et al., "LEO Satellite Constellations for 5G and Beyond: How Will They Reshape Vertical Domains?," in IEEE Com-munications Magazine, vol. 59, no. 7, pp. 30-36, July 2021, doi: 10.1109/MCOM.001.2001081

[29] X. Lin, S. Rommer, S. Euler, E. A. Yavuz and R. S. Karlsson, "5G from Space: An Overview of 3GPP Non-Terrestrial Networks," in IEEE Communications Standards Magazine, vol. 5, no. 4, pp. 147-153, December 2021, doi: 10.1109/MCOMSTD.011.2100038.

[30] R. Ding et al., "5G Integrated Satellite Communication Systems: Architectures, Air Interface, and Standardization," 2020 In-ternational Conference on Wireless Communications and Signal Processing (WCSP), Nanjing, China, 2020, pp. 702-707, doi: 10.1109/WCSP49889.2020.9299757.

[31] M. De Sanctis, E. Cianca, G. Araniti, I. Bisio and R. Prasad, "Satellite Communications Supporting Internet of Remote Things," in IEEE Internet of Things Journal, vol. 3, no. 1, pp. 113-123, Feb. 2016, doi: 10.1109/JIOT.2015.2487046.

[32] ESA Study: “Next-Generation Telecommunication Payloads based on Photonic Technologies”; Final Report; ESA Contract N° 22560/09/NL/AD,6/12/2011.

[33] ESA Study: "Roadmap for the Introduction of Photonic Technologies Based Payloads"; Final Report; ESA Contract N° 4000111857/14/NL/WE, Document n. TNO-PTLC-0007-TASI-2PRM; 6/09/2016.

[34] M. Sotom, M. Aveline, R. Barbaste, B. Benazet, A. Le Kernec, J. Magnaval, M. Picq, “Flexible Photonic payload for broadband telecom satellites: from concepts to demonstrators”, International Conference on Space Optics – ICSO 2016, 18-21 October 2016, Biarritz, France.

[35] C. Ciminelli, M. N. Armenise, F. Dell'Olio. Photonics in space: advanced photonic devices and systems. World Scientific, 2016.

[36] Hsu, Chung-Yu, Gow-Zin Yiu, and You-Chia Chang. 2022. "Free-Space Applications of Silicon Photonics: A Review" Mi-cromachines 13, no. 7: 990. https://doi.org/10.3390/mi13070990

[37] M. Krainak, M. Stephen, E. Troupaki, S. Tedder, B. Reyna, J. Klamkin, H. Zhao, B. Song, J. Fridlander, M. Tran, J. E. Bowers, K. Bergman, M. Lipson, A. Rizzo, I. Datta, N. Abrams, S. Mookherjea, S. T. Ho, Q. Bei, Y. Huang, Y. Tu, B. Moslehi, J. Harris, A. Matsko, A. Savchenkov, G. Liu, R. Proietti, S. J. B. Yoo, L. Johansson, C. Dorrer, F. R. Arteaga-Sierra, J. Qiao, S. Gong, T. Gu, O. J. Ohanian III, X. Ni, Y. Ding, Y. Duan, H. Dalir, R. T. Chen, V. J. Sorger, T. Komljenovic, "Integrated photonics for NASA applications," Proc. SPIE 10899, Components and Packaging for Laser Systems V, 108990F (4 March 2019); https://doi.org/10.1117/12.2509808

[38] "Preliminary IoV/IoD Scenarios Design Document – PART 2 - Photonic Hosted Payload"; H2020 E.C: Frame, topic: COMPET-05-2014 – IOV/IOD; Project "GOTOFLY! Boosting the European innovative Satellite Technologies with In Orbit Demonstration", 6 June 2016.

[39] D3 Candidate Payload Architectures and Key Technologies, 29/09/2017, ESA Contract No. 4000119211/16/NL/EM "Towards the 100 kW communications satellite".

[40] V. Schena, F. Finocchiaro, S. Vono, M. A. Feudale, J-D Gayrard, M. Sotom, M. Aveline; "GOTOFLY! Project: IOD/IOV Mission Scenario for a Hosted Photonic SATCOM Payload"; Proceedings; 22nd Ka and Broadband Communications Conference, Cleveland, Ohio, USA, October 17 - 20, 2016.

[41] S. Vono, M. Sotom, et al.; "Towards Telecommunication Payloads with Photonic Technologies"; International Conference on Space Optics (ICSO) 2014; Tenerife, Canary Islands, Spain; 7 - 10 October 2014.

[42] ESA Study: "Next-Generation Telecommunication Payloads based on Photonic Technologies"; Final Report; ESA Contract N° 22560/09/NL/AD, 6/12/2011.

[43] ESA Study: "Roadmap for the Introduction of Photonic Technologies Based Payloads"; Final Report; ESA Contract N° 4000111857/14/NL/WE, Document n. TNO-PTLC-0007-TASI-2PRM; 6/09/2016.

[44] J. Anzalchi, J. Wong, T. Verges, O. Navasquillo, T. Mengual, M. A. Piqueras, E. Prevost, K. Ravel, N. Parsons, M. Enrico, J. Bauwelink, M. Vanhoecke, A. Vannucci, M. Tienforti,

"Towards Demonstration of Photonic Payload for Telecom Satellites", International Conference on Space Optics – ICSO 2018, 9-12 October 2018, Chaina, Greece.

[45] L. Rodio, V. Schena, M. Grande, G. Calò, A. D'Orazio, "Microwave-photonic technologies for satellite telecommunication payloads: a focus on photonic RF frequency conversion", 2021 IEEE 8th International Workshop on Metrology for AeroSpace (MetroAeroSpace), 23-25 June 2021, Naples, Italy.

[46] J. Capmany, B. Ortega, D. Pastor, "A Tutorial on Microwave Photonic Filters", Journal of Lightwave Technology, Vol. 24, No. 1, January 2006.

[47] G. Papadimitriou, C. Papazoglou, A. Pomportsis, "Optical Switching: Switch Fabrics, Techniques, and Architectures", IEEE Journal on Lightwave Technology, Vol. 21, N. 2, February 2003

[48] N.F. de Rooij, S. Gau S.Gautsch, D. Briand, C. Marxer, G. Mileti,W. Noell, H. Shea, U. Staufer and B. van der Schoot, "MEMS for Space", IEEE Transducers 2009, Denver, CO, USA, June 21-25, 2009.

[49] Guray Acar, Daniel Arapoglou, Emiliano Re, Angelo Altamura, Alberto Mengali, Wael El-Dali, Monica Politano, Christopher Vasko, Haraldt Hauschildt, Josep Perdigues, Vincenzo Schena, Luca Rodio, Alberto Pandolfi, Peter Schwaderer, Garima Pandey, Ian Petersen, Joern Streppel, Klaus Schoenherr, "HydRON Vision: preparation towards a flight demonstration," Proc. SPIE 12777, International Conference on Space Optics — ICSO 2022, 127773W (12 July 2023); https://doi.org/10.1117/12.2690569.

[50] L. Rodio, V. Schena, M. Grande, G. Calò and A. D'Orazio, "Microwave-photonic technologies for satellite telecommunication payloads: a focus on photonic RF frequency conversion," 2021 IEEE 8th International Workshop on Metrology for AeroSpace (MetroAeroSpace), Naples, Italy, 2021, pp. 154-158, doi: 10.1109/MetroAeroSpace51421.2021.9511777.

[51] L. Rodio, V. Schena, M. Grande, G. Calò and A. D'Orazio, "Photonic multi-frequency down conversion in hybrid microwave-photonic SATCOM payload," 2022 ELEKTRO (ELEKTRO), Krakow, Poland, 2022, pp. 1-5, doi: 10.1109/ELEKTRO53996.2022.9803466.

[52] P. Li, W. Pan, X. Zou, S. Pan, B. Luo, L. Yan, "High-Efficiency Photonic Microwave Downconversion With Full-Frequency-Range Coverage", IEEE Photonics Journal, Volume 7, Number 4, August 2015, DOI: 10.1109/JPHOT.2015.2448522.

[53] Z. Tang, Y. Li, J. Yao, S. Pan, "Photonic-Based Microwave Frequency Mixing: Methodology and Applications", Laser Photonics Rev. 2020, 14, 1800350.

[54] S. A. Pappert, R. Helkey, R. T. Logan, “Photonic link techniques for microwave frequency conversion”, in RF Photonic Technology in Optical Fiber Links, W. S. C. Chang (Ed.), Cambridge University Press (2002).

[55] Z. Tang, S. Pan, “A Reconfigurable Photonic Microwave Mixer”, 2014 International Topical Meeting on Microwave Photonics (MWP) and the 2014 9th Asia-Pacific Microwave Photonics Conference (APMP).

[56] D. A. Fofanov, T. N. Bakhvalova, A. V. Alyoshin, M. E. Belkin, A. S. Sigov, “Microwave-Photonics Frequency Up-Converter for Telecom and Measurement Equipment”, IOP Conf. Series: Materials Science and Engineering 524 (2019) 012006, doi: 10.1088/1757-899X/524/1/012006.

[57] Y. Ji, H. Li, M. Tian, C. Gong, Y. Wei, “Microwave Photonics Down Conversion Based on Optical Frequency Comb”, 2020 IEEE 5th Optoelectronics Global Conference (OGC), 7-11 Sept. 2020.

[58] J. Min, Z. Zeng, Y. Su, Z. Zhang, L. Zhang, Y. Liu, “Microwave Photonic Frequency Conversion System Based on a Dual-loop Optoelectronic Oscillator for B5G/6G Communication”, 2021 19th International Conference on Optical Communications and Networks (ICOCN), DOI: 10.1109/ICOCN53177.2021.9563718.

[59] C. G. Bottenfield, M. Hoff, V. A. Thomas, A. Winoto, Y. Zhou, A. Bhardwaj, G. E. Hoefler, R. DeSalvo, S. E. Ralph, “High Performance Microwave Photonic Downconversion in a Commercial InP Platform”, 2021 Optical Fiber Communications Conference and Exhibition (OFC), 6-10 June 2021.

[60] C. G. Bottenfield, S. E. Ralph, “High-Performance Fully Integrated Silicon Photonic Microwave Mixer Subsystems, Journal of Lightwave Technology, Vol. 38, No. 19, October 1, 2020.

[61] Z. Tang, F. Zhang, D. Zhu, X. Zou, and S. Pan, “A Photonic Frequency Downconverter based on a Single Dual-Drive Mach-Zehnder Modulator”, IEEE International Topical Meeting on Microwave Photonics, Alexandria, Virginia, USA, October 28-31, 2013, p. 150.

[62] Y. Gao, A. Wen, Z. Tu, W. Zhang, and L. Lin, “Simultaneously photonic frequency downconversion, multichannel phase shifting, and IQ demodulation for wideband microwave signals”, Opt. Lett. 41, 4484 (2016).

[63] V. R. Pagan and T. E. Murphy, “Electro-optic millimeter-wave harmonic downconversion and vector demodulation using cascaded phase modulation and optical filtering”, Opt. Lett. 40, 2481 (2015).

[64] E. H. W. Chan and R. Minasian, “Microwave Photonic Downconverter With High Conversion Efficiency”, J. Lightwave Technol. 30, 3580 (2012).

[65] D. Zhu, S. Pan, S. Cai, and D. Ben, "High-Performance Photonic Microwave Downconverter Based on a Frequency-Doubling Optoelectronic Oscillator", J. Lightwave Technol. 30, 3036 (2012).

[66] Z. Shi, S. Zhu, M. Li, N. Zhu, and W. Li, “Reconfigurable microwave photonic mixer based on dual-polarization dual-parallel Mach–Zehnder modulator”, Opt. Commun. 428, 131 (2018).

[67] G. Charalambous, S. Iezekiel, “Microwave Photonic Frequency Generation and Conversion Unit Design for Ka-band Satellite Payloads”, International Conference on Space Optics - ICSO 2021, Virtual Conference, 30 March-2 April 2021.

[68] J. Yin, Y. Jiang, K. Xu, F. Yin, J. Li, “A Flexible Microwave Photonic Frequency Conversion Scheme for Satellite Repeater Applications”, 2014 Asia Communications and Photonics Conference (ACP), 11-14 Nov. 2014.

[69] T. Lin, S. Zhao, Z. Zhu, X. Li, K. Qu, “Photonic Microwave Multi-band Frequency Conversion Scheme Based on Dual-OFCs for Satellite Communication”, 2016 15th International Conference on Optical Communications and Networks (ICOCN), 24-27 Sept. 2016.

[70] Yin Jie, Dong Tao, Zhang Bin, Hao Yan, Cao Guixing, Cheng Zijing, Xu Kun, Zhou Yue, Dai Jian, “Multi-band microwave photonic satellite repeater scheme employing intensity Mach-Zehnder modulators”, The Journal of China Universities of Posts and Telecommunications, April 2017, 24(2): 89–95.

[71] S. Zhu, X. Fan, M. Li, N. H. Zhu, W. Li, “Microwave photonic frequency down-conversion and channel switching for satellite communication”, Optics Letters, Vol. 45, No. 18, 15 September 2020.

[72] Z. Wang, X. Wang, Qi. Zhang, X. Xin, R.Gao, Y. Tao, X.Sheng, Q.Tian, F.Tian, Y.Wang, W. Zhang, H.Chang, D.Chen, J.Qian, "A satellite on-board processing scheme based on photon frequency conversion," Proc. SPIE 11763, Seventh Symposium on Novel Photoelectronic Detection Technology and Applications, 117636N (12 March 2021), Kunming, China; doi: 10.1117/12.2587374.

[73] X. Deng, Y. Zhao, X. Qin, H. Wu, Q. Tan, J.Hui, "Research on microwave photonics mixer technology of HTS communication satellite," Proc. SPIE 11763, Seventh Symposium on Novel Photoelectronic Detection Technology and Applications, 117636O (12 March 2021), Kunming, China; doi: 10.1117/12.2587377.

[74] V. C. Duarte, J. G. Prata, C. F. Ribeiro, R. N. Nogueira, G.Winzer,L.Zimmermann, R.Walker, S.Clements, M.Filipowicz, M. Napierała, T.Nasiłowski, J. Crabb, M. Kechagias, L. Stampoulidis, J.Anzalchi,M.V. Drummond, "Modular coherent photonic-aided payload receiver for communications satellites", Nature Communications, 10, art. n.1984, 2019.

[75] S. Betti, M. Giaconi, "Comunicazioni Ottiche", 2003, Aracne Editrice.

[76] L. Rodio, V. Devito, M. Grande, G. Calò and A. D'Orazio, "Design of an optical Butler matrix for beamforming in satellite communications," 2022 IEEE 9th International Workshop on Metrology for AeroSpace (MetroAeroSpace), Pisa, Italy, 2022, pp. 436-440, doi: 10.1109/MetroAeroSpace54187.2022.9855971.

[77] Vidal B., Mengual T., Martí J., Gomes Nathan J., :Fast Optical Beamforming Architectures for Satellite-Based Applications, Advances in Optical Technologies, 2012, Volume 2012 |Article ID 385409 | https://doi.org/10.1155/2012/385409.

[78] Tessema N.M., Cao Z., Tangdiongga E., Koonen A.M.J.: Optical beam forming system for satellite communication, In S.M.Garcia-Bianco, K.J.Boller, M.A.Sefunc, D.Geuzebroek (editors), Proceedings of the 19th Annual Symposium of the IEEE Photonics Benelux Chapter, 3-4 November 2014, Ensched, The Netherlands (biz 121-124). Twente University.

[79] Kim, SM., Baek, MW., Nahm, S.H. Visible light communication using TDMA optical beamforming. J Wireless Com Network, 2017, 56, https://doi.org/10.1186/s13638-017-0841-3.

[80] C. Tsokos, E. Mylonas, P. Groumas, L. Gounaridis, H. Avramopoulos and C. Kouloumentas, "Optical Beamforming Network for Multi-Beam Operation With Continuous Angle Selection," in IEEE Photonics Technology Letters, vol. 31, no. 2, pp. 177-180, 15 Jan.15, 2019, doi: 10.1109/LPT.2018.2889411.

[81] Y. M. Meleshin; A. A. Biryuk; A. Y. Sheremet; Z. V. Merkulova; V. K. Tsvetkov; The advantages of microwave photonic beamforming in broadband APAA; 2018 IEEE Conference of Russian Young Researchers in Electrical and Electronic Engineering (EIConRus); 29 Jan. - 1 Feb. 2018; DOI: 10.1109/EIConRus.2018.8317426.

[82] J. Anzalchi, R. Perrott, K. Latunde-Dada, R. M. Oldenbeuving, C.G.H. Roeloffzen, P.W.L. Van Dijk, M. Hoekman, H. Leeuwis, A. Leinse, Optical beamforming based on microwave photonic signal processing, International Conference on Space Optics (ICSO 2016), Biarritz, France, 18–21 October 2016.

[83] G. Barb, M. Otesteanu, F. Alexa and A. Ghiulai, "Digital Beamforming Techniques for Future Communications Systems," 2020 12th International Symposium on Communication Systems, Networks and Digital Signal Processing (CSNDSP), 2020, pp. 1-4, doi: 10.1109/CSNDSP49049.2020.9249607.

[84] C. N. Barati, S. Dutta, S. Rangan, A. Sabharwal, Energy and Latency of Beamforming Architectures for Initial Access in mmWave Wireless Networks. Journal of the Indian Institute of Science 100, 281–302 (2020). https://doi.org/10.1007/s41745-020-00170-9.

[85] Hansen R.C.: Phased array antennas, 2nd Edition, John Wiley & Sons, New Jersey 2009.

[86] Ajioka J.S., McFarland J.L.: "Beam forming feeds", Antenna Handbook: Theory, Applications and Design, Y.T.Lo and S.W.Lee eds, Van Nostrand Reinhold, New York, 1988.

[87] Butler, J. L. and R. Lowe, "Beam forming matrix simplifies design of electronically scanned antennas," Electronic Design, Vol. 9, 170-173, Apr. 1961.

[88] Blass, J., "Multidirectional antenna — A new approach to stacked beams," IRE Int. Conf. Record, Vol. 8, 48-50, 1960.

[89] Nolen, J., "Synthesis of multiple beam networks for arbitrary illuminations," Ph.D. Dissertation, Radio Division, Bendix Corp., Baltimore, MD, Apr. 1965.

[90] L. Shevada, H. D. Raut, R. Malekar, S. Kumar, Comparative Study of Different Beamforming Techniques for 5G: A Review, in: Ranganathan, G., Chen, J., Rocha, Á. (eds) Inventive Communication and Computational Technologies. Lecture Notes in Networks and Systems, vol 145. Springer, Singapore. https://doi.org/10.1007/978-981-15-7345-3_50.

[91] N. S. M. Suhaimi, N. M. Mahyuddin, Review of Switched Beamforming, Networks for Scannable Antenna Application towards Fifth Generation (5G) Technology; International Journal of Integrated Engineering, Vol. 12 No. 6 (2020) 62-70, DOI: https://doi.org/10.30880/ijie.2020.12.06.008.

[92] C.-H. Tseng, C.-J. Chen, and T.-H. Chu, "A low-cost 60-GHz switched beam patch antenna array with Butler matrix network," IEEE Antennas Wireless Propag. Lett., vol. 7, pp. 432-435, 2008.

[93] B. Cetinoneri, Y. A. Atesal, and G. M. Rebeiz, "An 8 × 8 Butler matrix in 0.13 μm in CMOS for 5-6-GHz multibeam applications," IEEE Trans. Microw. Theory Techn., vol. 59, no. 2, pp. 295-301, Feb. 2011.

[94] R. D. Cerna and M. A. Yarleque, "A 3D compact wideband 16 × 16 Butler matrix for 4G/3G applications," in IEEE MTT-S Int. Microw. Symp. Dig., Dec. 2018, pp. 16-19.

[95] Q. Shao, F. C. Chen, Q. X. Chu, and M. J. Lancaster, "Novel filtering 180° hybrid coupler and its application to 2 × 4 filtering Butler matrix," IEEE Trans. Microw. Theory Techn., vol. 66, no. 7, pp. 3288-3296, Jul. 2018.

[96] M. Koubeissi, C. Decroze, T. Monediere, and B. Jecko, "Switched-beam antenna based on novel design of Butler matrices with broadside beam," Electron. Lett., vol. 41, no. 20, pp. 1097-1098, Sep. 2005.

[97] P. Kaminski, K. Wincza, and S. Gruszczynski, "Switched-beam antenna array with broadside beam fed by modified Butler matrix for radar receiver application," Microw. Opt. Technol. Lett., vol. 56, no. 3, pp. 732-735, Mar. 2014.

[98] Y. Cao, K.-S. Chin, W. Che, W. Yang, and E. S. Li, "A compact 38 GHz multibeam antenna array with multifolded Butler matrix for 5G applications," IEEE Antennas Wireless Propag. Lett., vol. 16, pp. 2996-2999, 2017.

[99] J.-W. Lian, Y.-L. Ban, C. Xiao, and Z.-F. Yu, "Compact substrate- integrated 4 × 8 Butler matrix with sidelobe suppression for millimeter- wave multibeam application," IEEE Antennas Wireless Propag. Lett., vol. 17, no. 5, pp. 928-932, May 2018.

[100] K. Wincza, K. Staszek, I. Slomian, and S. Gruszczynski, "Scalable multibeam antenna arrays fed by dual-band modified Butler matrices," IEEE Trans. Antennas Propag., vol. 64, no. 4, pp. 1287-1297, Apr. 2016.

[101] S. Karamzadeh, V. Rafii, M. Kartal, and B. S. Virdee, "Compact and broadband 4 × 4 SIW Butler matrix with phase and magnitude errorreduction," IEEE Microw. Wireless Compon. Lett., vol. 25, no. 12, pp. 772-774, Dec. 2015.

[102] A. Moscoso-Martir, I. Molina-Fernandez, and A. Ortega-Monux, "Wide-band slot-coupled Butler matrix," IEEE Microw. Wireless Compon. Lett.,vol. 24, no. 12, pp. 848-850, Dec. 2014.

[103] Y. Wang, K. Ma, and Z. Jian, "A low-loss Butler matrix using patch element and honeycomb concept on SISL platform," IEEE Trans.Microw. Theory Techn., vol. 66, no. 8, pp. 3622-3631, Aug. 2018.

[104] K. Tekkouk, J. Hirokawa, R. Sauleau, M. Ettorre, M. Sano, and M. Ando,"Dual-layer ridged waveguide slot array fed by a Butler matrix with sidelobe control in the 60-GHz band," IEEE Trans. Antennas Propag., vol. 63, no. 9, pp. 3857-3867, Sep. 2015.

[105] H. Ren, B. Arigong, M. Zhou, J. Ding, and H. Zhang, "A novel design of 4 × 4 Butler matrix with relatively flexible phase differences," IEEE Antennas Wireless Propag. Lett., vol. 15, pp. 1277-1280, 2016.

[106] C.-C. Chang, R.-H. Lee, and T.-Y. Shih, "Design of a beam switching/steering Butler matrix for phased array system," IEEE Trans. Antennas Propag., vol. 58, no. 2, pp. 367-374, Feb. 2010.

[107] H. N. Chu and T.-G. Ma, "An extended 4 × 4 Butler matrix with enhanced beam controllability and widened spatial coverage," IEEE Trans. Microw. Theory Techn., vol. 66, no. 3, pp. 1301-1311, Mar. 2018.

[108] Li, W.-R., C.-Y. Chu, K.-H. Lin, and S.-F. Chang, "Switched-beam antenna based on modified Butler matrix with low sidelobe level", Electronics Letters, Vol. 40, No. 5, 290-292, Mar. 2004.

[109] Shelton, J. P., "Reduced sidelobes for Butler-matrix-fed linear arrays," IEEE Trans. Antennas Propagat., Vol. 17, No. 5, 645-647, Sep. 1969.

[110] J. T. Gallo and R. DeSalvo, "Experimental demonstration of optical guided-wave butler matrices," IEEE Trans. Microw. Theory Techn., vol. 45, no. 8, pp. 1501–1507, Aug. 1997.

[111] W. Charczenko, M. R. Surette, P. J. Matthews, H. Klotz, and A. R. Mickelson, "Integrated optical Butler matrix for beam forming in phased- array antennas," in OE/LASE'90, 14–19 Jan. 1990, pp. 196–206.

[112] D. Madrid, B.Vidal, A.Martinez, V.Polo, J.L.Polo, J.L.Corral, J.Marti: "A novel 2N beams heterodyne optical beamforming architecture based on NxN optical Butler matrices," in Proc. IEEE MTT-S Int. Microw. Symp. Dig., 2002, pp. 1945–1948.

[113] Huiyuan Liu, Xiang Liu, Frank Effenberger, Naresh Chand, Xiaofeng Qi. and Guifang Li: Optical Implementation of Butler Matrix for Hardware-Efficient Multiuser Beamforming, IEEE Photonics Journal, Volume 10, Number 2, April 2018.

[114] S. Durante, L. Rodio, V. Schena, G. Calò, A. D'Orazio and V. Ferrara, "A system demonstration of optical circuit switching in a space-based WDM Optical Transport Network," 2023 IEEE 10th International Workshop on Metrology for AeroSpace (MetroAeroSpace), Milan, Italy, 2023, pp. 633-637, doi: 10.1109/MetroAeroSpace57412.2023.10190029.

[115] TAO - Towards the All Optical satellite communication system, Public Report, 2018, Airbus, Nokia, Cilas.

[116] S. Bregni, G. Guerra, and A. Pattavina, "State of the art of optical switching technology for all-optical networks," in Communications World. Rethymo, Greece: WSES Press, 2001.

[117] A. Dugan, L. Lightworks, and J.-C. Chiao, "The optical switching spectrum: A primer on wavelength switching technologies", Telecommunications Magazine, May 2001.

[118] G. I. Papadimitriou, C. Papazoglou and A. S. Pomportsis, "Optical switching: switch fabrics, techniques, and architectures," in Journal of Lightwave Technology, vol. 21, no. 2, pp. 384-405, Feb. 2003, doi: 10.1109/JLT.2003.808766.

[119] X. Ma and G.S. Kuo, "Optical switching technology comparison: optical MEMS vs. other technologies," in IEEE Communications Magazine, vol. 41, no. 11, pp. S16-S23, Nov. 2003, doi: 10.1109/MCOM.2003.1244924.

[120] D. Poudereux, J. Barbero, J. M. G. Tijero, I. Esquivias, I. Mackencie, "Evaluation of Optical Switches for Space Applications," Proc. SPIE 11180, International Conference on Space Optics - ICSO 2018, 111807H (12 July 2019); https://doi.org/10.1117/12.2536188.

[121] K. Ravel, C. Koechlin, E. Prevost, T. Bomer, R. Poirier, L. Tonck, G. Guinde, M. Beaumel, N. Parsons, M. Enrico, S. Barker, "Optical switch matrix development for new concepts of photonic based flexible telecom payloads," Proc. SPIE 11180, International Conference on Space Optics – ICSO 2018, 111803H (12 July 2019); https://doi.org/10.1117/12.2536044.

[122] ESA Contract n.: 4000136543/21/NL/CLP HydRON DEMOnstration System (DS) PHASE A/B1 (HyDEMO) - Inputs for CMIN22.

[123] International Telecommunication Union, ITU-T G.694.1 (10/2020), Series G: Transmission Systems and Media, Digital Systems and Networks. Transmission media and optical systems characteristics. Spectral grids for WDM applications: DWDM frequency grid.